



pH dependence of cyanide and imidazole binding to the heme domains of *Sinorhizobium meliloti* and *Bradyrhizobium japonicum* FixL



Anil K. Bidwai, Angela J. Ahrendt, John S. Sullivan, Lidia B. Vitello, James E. Erman*

Department of Chemistry and Biochemistry, Northern Illinois University, DeKalb, IL 60115, United States of America

ARTICLE INFO

Article history:

Received 18 June 2015

Received in revised form 25 September 2015

Accepted 5 October 2015

Available online 22 October 2015

Keywords:

FixL

Heme domains

Cyanide binding

Imidazole binding

Equilibrium dissociation constant

Kinetics

ABSTRACT

Equilibrium and kinetic properties of cyanide and imidazole binding to the heme domains of *Sinorhizobium meliloti* and *Bradyrhizobium japonicum* FixL (*SmFixLH* and *BjFixLH*) have been investigated between pH 5 and 11. K_D determinations were made at integral pH values, with the strongest binding at pH 9 for both ligands. K_D for the cyanide complexes of *BjFixLH* and *SmFixLH* is 0.15 ± 0.09 and 0.50 ± 0.20 μM , respectively, and 0.70 ± 0.01 mM for imido-*BjFixLH*. The association rate constants are pH dependent with maximum values of 443 ± 8 and 252 ± 61 $\text{M}^{-1} \text{s}^{-1}$ for cyano complexes of *BjFixLH* and *SmFixLH* and $(5.0 \pm 0.3) \times 10^4$ and $(7.0 \pm 1.4) \times 10^4$ $\text{M}^{-1} \text{s}^{-1}$ for the imidazole complexes. The dissociation rate constants are essentially independent of pH above pH 5; $(1.2 \pm 0.3) \times 10^{-4}$ and $(1.7 \pm 0.3) \times 10^{-4}$ s^{-1} for the cyano complexes of *BjFixLH* and *SmFixLH*, and (73 ± 19) and (77 ± 14) s^{-1} for the imidazole complexes. Two ionizable groups in FixLH affect the rate of ligand binding. The more acidic group, identified as the heme 6 propionic acid, has a $\text{p}K_a$ of 7.6 ± 0.2 in *BjFixLH* and 6.8 ± 0.2 in *SmFixLH*. The second ionization is due to formation of hydroxy-FixLH with $\text{p}K_a$ values of 9.64 ± 0.05 for *BjFixLH* and 9.61 ± 0.05 for *SmFixLH*. Imidazole binding is limited by the rate of heme pocket opening with maximum observed values of 680 and 1270 s^{-1} for *BjFixLH* and *SmFixLH*, respectively.

© 2015 Elsevier Inc. All rights reserved.

1. Introduction

Studies of ligand binding to heme proteins provide crucial information concerning the structural basis for heme protein activity [1]. The heme iron exists in a number of redox states that bind distinctly different ligands. Among the Fe(II) heme ligands, O_2 , CO, and NO are most important, while Fe(III) heme ligands include cyanide, azide, fluoride, and imidazole. The Fe(III) heme ligands tend to be weak acids or bases and the binding of these ligands are often pH dependent, providing information on the discrimination between neutral and charged forms of the ligand, as well as being sensitive reporters of the acid/base chemistry, the electrostatic environment, and the accessibility of the heme.

An important class of heme proteins is the heme-based sensor proteins that function by detecting the presence of such small diatomic molecules as O_2 , CO, and NO [2]. This class includes the FixL protein in the nitrogen-fixing bacteria *Rhizobia*. FixL is an oxygen sensing protein that works in tandem with the regulator protein FixJ as part of a classic

bacterial two-component regulatory system [3,4]. In the presence of O_2 , these two proteins ultimately inhibit transcription of the nitrogen-fixing genes *nifA* and *fixK* [5].

FixL from *Sinorhizobium meliloti* (formerly *Rhizobium meliloti*), *SmFixL*, contains three functional domains, an N-terminal transmembrane domain, a central heme-sensor domain, and a C-terminal histidine kinase domain [6,7]. The FixL from *Bradyrhizobium japonicum* (*BjFixL*) is soluble, lacking the transmembrane domain [8]. The activity of the kinase domain responds to the spin-state of the heme iron in the sensor domain [9]. In the unligated Fe(II) and Fe(III) forms of FixL, the kinase activity is maximal, while binding a strong-field ligand such as O_2 to the Fe(II) heme or cyanide to the Fe(III) state inactivates the kinase activity. Ligand binding induces a conformational change in the heme domain that is relayed to the kinase domain causing the transition between active and inactive states. Currently, twenty-one structures of the heme domains of *BjFixL* and *SmFixL* have been deposited in the protein data bank including those of the unligated Fe(II) and Fe(III) states as well as those of the O_2 , CO, NO, CN^- , imidazole, and 1-methylimidazole complexes documenting the conformational changes associated with ligand binding in these proteins [10–18].

The rates of ligand binding to the heme domains of both *BjFixL* and *SmFixL* have been determined for O_2 and CO to the Fe(II) state and for NO, azide, cyanide, fluoride, imidazole, and 4-methylimidazole to the Fe(III) state, generally in the pH region 7 to 8 [14,16,19–27]. Both O_2 and CO bind to the FixLs at a slower rate than they bind to deoxy-moglobin. Cyanide binding to the Fe(III) state of the FixLs is slower

Abbreviations: FixL, heme sensor protein found in nitrogen-fixing bacteria; FixLH, truncated version of FixL containing the soluble heme domain; *BjFixL*, FixL from *Bradyrhizobium japonicum*; *BjFixLH*, FixLH from *Bradyrhizobium japonicum*; *SmFixL*, FixL from *Sinorhizobium meliloti*; *SmFixLH*, FixLH from *Sinorhizobium meliloti*; CcP, cytochrome c peroxidase; MetMb, metmyoglobin; HP6, propionic acid at heme position 6; HP7, propionic acid at heme position 7.

* Corresponding author.

E-mail address: jerman@niu.edu (J.E. Erman).

than binding to metmyoglobin but both NO and imidazole bind to FixL at a faster rate than to metmyoglobin. Winkler et al. [21] found that the affinities of the basic ligands for metFixL correlated with the ligand pK_a values and that the association rate constants following the reverse trend. The observation that bulky ligands such as imidazole and 4-methylimidazole bound faster than the smaller cyanide and fluoride ions suggested that steric factors were not rate-limiting but rather that the rates of bond formation and deprotonation of the ligand within the apolar heme pocket were the dominant factors in complex formation.

Ligand binding to the Fe(III) state of the heme sensors is relatively uncharacterized compared to representatives of other major classes of heme proteins. FixL has a novel heme-binding fold, an apolar heme pocket, and undergoes significant structural change upon ligand binding [10]. The primary goal of this study is to investigate the pH dependence of cyanide and imidazole to the heme domain of FixL (FixLH) and compare the mechanism of ligand binding to FixLH with binding to the other major classes of heme proteins. Due to the coupling of significant conformational changes with ligand binding, the FixLH studies may provide additional, unique, insight into how protein structure can modulate the chemical reactivity of the heme group.

2. Materials and methods

2.1. Cloning, expression, and purification of the FixL heme domains

The heme domain of BjFixL was cloned by amplifying codons 140–270 of the FixL gene using genomic DNA from *B. japonicum* as the template for PCR. An NdeI recognition site was introduced at the 5' end and an EcoRI site introduced at the 3' end. NdeI/EcoRI digests were ligated into the Novagene vector pET-24b(+) under the control of the T7 promoter to produce the expression construct named pET-24b(+)/BjFixLH.

Escherichia coli strain TG1 with the plasmid pEM130 coding for ampicillin resistance and for the *S. meliloti* FixLN and FixJ proteins was provided by Andrew Hansen of Northern Illinois University. The heme domain of SmFixL was amplified by PCR using primers that introduced NdeI and BamHI restriction sites at the 5' and 3' ends of the DNA. The amplified fragments were ligated into pJES307 to produce an expression vector named pJES307/SmFixLH. DNA sequencing indicated that the cloned SmFixLH corresponded to residues 123 to 260 of SmFixL.

The plasmid pET-24b(+)/BjFixLH was transformed into *E. coli* strain BL21(DE3) and liter cultures grown at 37 °C in TB medium containing 50 µg/mL ampicillin. Expression was induced by 1 mM IPTG at OD₆₀₀ between 1.0 and 1.2. The induced culture was grown overnight at 28 °C. Cells were harvested and lysed in a French Press. The supernatant containing BjFixLH was applied to a gel-filtration column, Sephadex G-75, and eluted with a buffer containing 20 mM potassium phosphate, 100 mM NaCl, pH 7.5. Fractions containing the protein were pooled and applied to a DEAE-Sepharose (FastFlow) column equilibrated with a 20 mM potassium phosphate buffer pH 8.0 and eluted with a 50–500 mM NaCl gradient over 200 mL. Purity of BjFixLH was determined by SDS-PAGE and UV-vis spectroscopy.

The plasmid pJES307/SmFixLH was transformed into *E. coli* strain BL21(DE3) and liter cultures grown at 37 °C in LB medium containing 50 µg/mL ampicillin. Expression was induced by 1 mM IPTG at OD₆₀₀ between 0.5 and 0.7. The induced culture was grown for a further 4–5 h for optimum protein expression. SmFixLH expresses predominantly in the insoluble fraction, and hence had to be isolated and purified by denaturation of inclusion bodies with 8 M urea and subsequent refolding of the protein. Cells were lysed by sonication and the insoluble protein was solubilized in 15 mL of Buffer A (20 mM Tris, 10 mM NaCl, 5% glycerol, 10 mM β-mercaptoethanol and 1 mM phenylmethylsulfonyl fluoride, pH 8.0) containing 8 M urea and 0.75 mM hemin. The solubilized mixture was dialyzed against two changes of Buffer A

containing hemin but no urea, followed by a third change against Buffer A without hemin. The dialysate was applied directly to a DEAE-Sepharose (FastFlow) column pre-equilibrated with Buffer A and eluted with a 10–300 mM NaCl gradient over 200 mL. Fractions containing SmFixLH were pooled and further purified by gel filtration on Sephadex G-75. Purity of SmFixLH was determined by SDS-PAGE and UV-vis spectroscopy.

MALDI-TOF mass spectrometry of the purified proteins indicated that the N-terminal methionine was removed from BjFixLH but that SmFixLH retained the N-terminal methionine.

2.2. Buffers

Between pH 4.0 and 5.5, buffers were 0.010 M acetate with sufficient KH₂PO₄ to adjust the ionic strength to 0.100 M. Between pH 5.5 and 8.0, the buffers were mixtures of KH₂PO₄ and K₂HPO₄ with a total ionic strength of 0.100 M. Between pH 8.5 and 10.5, the buffers were 0.010 M glycine with added K₂HPO₄ to adjust the ionic strength to 0.100 M. Between pH 11.0 and 11.5, the buffers were mixtures of K₂HPO₄ and K₃PO₄ with a total ionic strength of 0.100 M.

2.3. Spectroscopic measurements and protein concentration determination

Electronic absorption spectra of protein solutions were determined using either a Varian/Cary Model 3E or a Hewlett Packard Model 8452A spectrophotometer. The extinction coefficients of BjFixLH and SmFixLH were determined using the pyridine hemochromogen method of Berry and Trumpower [28].

2.4. Equilibrium constant determinations

Spectroscopic changes associated with formation of the cyanide and imidazole complexes enabled monitoring of complex formation. Determination of the equilibrium constants was done by titrating ~10 µM protein with increasing concentrations of buffered ligand solution until saturation was reached. The solutions were generally incubated overnight to assure equilibrium had been attained. Equilibrium studies were carried out at integral pH intervals between 4 and 11 for cyanide and between pH 6 and 11 for imidazole, 25 °C.

2.5. Transient-state kinetic measurements

The rates of cyanide and imidazole binding were determined using an Applied Photophysics Ltd. stopped-flow instrument. The reactions were monitored at the wavelength of maximum difference between the ligand-free and ligand-bound states, 426 nm for cyanide binding and 418 nm for imidazole binding. Reactions were carried out under pseudo-first order conditions with excess ligand. Protein concentrations were typically ~1 µM. Observed rate constants were determined at a minimum of five different ligand concentrations at each pH with the ligand concentration varying by at least a factor of five for each experiment. A minimum of 10 individual traces of absorbance change versus time were acquired at each ligand concentration allowing the mean value of the observed rate constant and its standard deviation to be determined. Kinetic studies were carried out at every half pH between pH 5 and 11 at 0.10 M ionic strength, 25 °C.

2.6. Data analysis

Data analysis was performed using SigmaPlot version 12.5. Equilibrium constants for both cyanide and imidazole binding were determined by fitting the change in absorbance to a single-site binding isotherm using non-linear least squares regression. The standard deviation in K_D was estimated from the fit of the data and averages 13% of K_D . The value of k_a for cyanide binding was determined from the slope of linear plots of k_{obs} versus the cyanide using linear least square regression. The

standard deviation of k_a was calculated from the fit and averages 9% of k_a . The value of k_d for cyanide dissociation was calculated from the product of K_D and k_a and has an average calculated standard deviation of 16%. The rate of imidazole binding saturates at high imidazole concentrations (Section 3.6). The value of k_{obs} was fit to a three parameter empirical equation using non-linear least squares regression with standard deviations of the parameters estimated from the fit. The standard deviation of P1, the apparent association rate constant, averages 26% and the average standard deviation for P2, the apparent dissociation rate constant, is 13%. Due to the long extrapolation to saturation, the standard deviation for P3, the parameter that describes the curvature of the k_{obs} plot, averages 47%.

3. Results

3.1. Spectroscopic properties of *BjFixLH* and *SmFixLH*

The electronic absorption spectra of both *BjFixLH* and *SmFixLH* are pH dependent. Spectra of *BjFixLH* at pH 7 and 11 are shown in Fig. 1. The spectrum of *SmFixLH* is nearly identical to that of *BjFixLH* and is shown in Fig. S1 of the Supplementary Data, Appendix A, provided with this article. Selected spectral parameters for both heme domains are collected in Table 1.

Plots of the absorbance change at the Soret maxim (395 nm) are shown as a function of pH in Fig. 2. The data were fit to the titration of a single ionizable group using non-linear least squares regression. Best-fit values for the apparent pK_a s are 9.64 ± 0.05 and 9.61 ± 0.05 for *BjFixLH* and *SmFixLH*, respectively. Spectra of the alkaline forms of the heme domains, attributed to hydroxide ion binding to the heme iron, were calculated from the pH 7 and 11 spectra using the appropriate pK_a values. Selected spectral parameters for *BjFixLH*-OH and *SmFixLH*-OH are collected in Table 1.

3.2. Equilibrium binding of cyanide to *BjFixLH* and *SmFixLH*

Addition of buffered cyanide solutions to the FixL heme domains causes large changes in the absorption spectrum of the protein. Spectral changes associated with cyanide binding to *BjFixLH* at pH 7.0 are shown in Fig. 3. The Soret maximum shifts from 395 nm to 423 nm with a 13% increase in intensity of the Soret band. Spectral changes associated with cyanide binding to *SmFixLH* at pH 7.0 are shown in Fig. S2 (Supplementary Data). Formation of the cyanide complexes of both FixLHs is essentially complete under the experimental

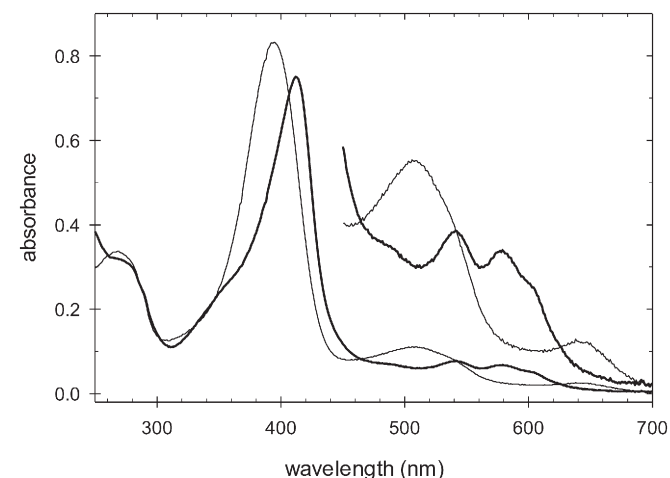


Fig. 1. The absorption spectra of *BjFixLH* at pH 7.0 (thin solid line) and at pH 11.0 (thick solid line).

conditions used to determine the spectra shown in Figs. 3 and S2. Selected spectroscopic parameters of the FixLH cyanide complexes are included in Table 1.

The spectrum of the cyano complex of *BjFixLH* is independent of pH between pH 5 and 11, with only a minor perturbation at pH 4, Fig. S3. The spectrum of the cyano complex of *SmFixLH* is independent of pH between 7 and 11. Below pH 7, there is a decrease in the intensity of the Soret band and a shift from 423 nm at pH 7 to 419 nm at pH 4, Fig. S4. Both *SmFixLH* and its cyano complex appear to be more susceptible to acid denaturation than *BjFixLH*. After overnight incubation, both *SmFixLH* and its cyanide complex were slightly turbid suggesting some denaturation had occurred at pH 4.

Cyanide titrations of the heme domains were monitored using the change in absorbance at 426 nm, the wavelength of maximum difference between FixLH and its cyanide complex. Identical aliquots of the heme domain were added to a series of test tubes containing buffered cyanide solutions of increasing ligand concentration. Samples were incubated overnight to assure complete equilibration. Plots of ΔA_{426} as a function of the total cyanide concentration are shown for both *BjFixLH* and *SmFixLH* at pH 7 in Fig. 4.

To determine the equilibrium dissociation constant, K_D , the data shown in Fig. 4 were fit to Eq. (1). In Eq. (1), P and L represent the total protein and total ligand concentrations,

$$\Delta A_{obs} = \frac{\Delta A_{max}}{2P} \left(B - \sqrt{B^2 - 4PL} \right) \quad (1)$$

respectively, and B is equal to $(P + L + K_D)$. ΔA_{max} is the maximum change in absorbance at infinite ligand concentration. Best-fit values for K_D at pH 7.0 are $(5.2 \pm 0.5) \mu\text{M}$ and $(10.4 \pm 0.9) \mu\text{M}$ for the *BjFixLH*-CN and *SmFixLH*-CN complexes, respectively.

K_D for both the *BjFixLH*-CN and *SmFixLH*-CN complexes were determined at integral pH values between pH 4 and 11. A plot of the negative logarithm of K_D ($\log K_A$) as a function of pH is shown in Fig. 5 for both *BjFixLH*-CN and *SmFixLH*-CN. The binding affinity for cyanide is strongest at pH 9 where K_D is $0.15 \pm 0.09 \mu\text{M}$ for *BjFixLH*-CN and $0.50 \pm 0.20 \mu\text{M}$ for *SmFixLH*-CN, Fig. S5. Values of K_D at all pH values are collected in Tables S1 and S2 for *BjFixLH*-CN and *SmFixLH*-CN, respectively. The solid lines through the data in Fig. 5 were calculated from a mechanism to be discussed below.

3.3. Equilibrium binding of imidazole to *BjFixLH*

The spectrum of the imidazole complex with *BjFixLH* at pH 7.0 is shown in Fig. 3. The Soret maximum shifts from 395 nm in the absence of imidazole to 415 nm in the presence of imidazole. The spectrum of the *BjFixLH*-imidazole complex is independent of pH between pH 6 and 11 with α , β , and Soret bands at 563, 534, and 415 nm, respectively, Table 1.

Equilibrium dissociation constants for the *BjFixLH*-imidazole complex were determined by titrating approximately $\sim 8 \mu\text{M}$ protein with increasing imidazole concentrations. Absorbance changes were monitored at 418 nm, the wavelength of maximum difference between the complex and the free protein. A titration at pH 8.0 is shown in Fig. S6. The best-fit value of K_D for the *BjFixLH*-imidazole complex at pH 8.0 is $1.9 \pm 0.1 \text{ mM}$, about 3 orders of magnitude weaker than for the cyanide complex.

The equilibrium dissociation constant for the *BjFixLH*-imidazole complex was determined at each half pH unit between pH 6 and 11. Values of K_D are collected in Table S3. Values of $-\log(K_D) = \log(K_A)$ are plotted as a function of pH in Fig. 5. The bell-shaped dependence of $-\log(K_D)$ indicates that at least two ionizable groups influence imidazole binding to *BjFixLH*. The data are best fit using the equilibrium association constant, K_A , rather than K_D and were fit to an empirical equation involving two ionizable groups with pK_a s designated pK_{a1}

Table 1
Spectroscopic parameters for *BjFixLH*, *SmFixLH*, and their hydroxide and cyanide complexes.

Protein	Protein λ (ϵ) ^b	δ band λ (ϵ) ^b	Soret band λ (ϵ) ^b	CT2 band ^a λ (ϵ) ^b	β band λ (ϵ) ^b	α band λ (ϵ) ^b	CT1 band ^a λ (ϵ) ^b
<i>BjFixLH</i>	269 (51)		395 (126)	508 (16.8)	535sh (13.02)		642 (3.8)
<i>SmFixLH</i>	269 (31)		395 (126)	510 (16.0)	536sh (12.8)		642 (3.4)
<i>BjFixLH-OH</i>	269sh (48)	360sh (41)	412 (114)	490sh (10.4)	541 (11.7)	578 (10.3)	605sh (7.5)
<i>SmFixLH-OH</i>	276sh (31)	356sh (40)	410 (110)	488sh (10.8)	539 (10.8)	578 (9.2)	602sh (8.0)
<i>BjFixLH-CN</i>	269 (53)	364 (39)	423 (142)	484sh (11.8)	540 (15.1)	574sh (11.4)	
<i>SmFixLH-CN</i>	274 (31)	364 (36)	423 (135)	488sh (10.5)	540 (14.3)	574sh (10.3)	
<i>BjFixLH-imid</i>	265 (59)	360sh (34)	415 (145)	485sh (9.8)	534 (13.8)	563 (12.1)	

^a CT1 and CT2 represent charge transfer bands. ^b λ , wavelength in nm. ϵ , extinction coefficient in $\text{mM}^{-1} \text{cm}^{-1}$; sh follows the value of λ if the band appears as a shoulder.

and pK_{a2} , Eq. (2). In Eq. (2), the values of K_A^{acid} , K_A^{neut} , and K_A^{base} are the limiting values of K_A at

$$K_A = \frac{K_A^{acid} \frac{[H^+]}{K_{a1}} + K_A^{neut} + K_A^{base} \frac{K_{a2}}{[H^+]}}{\left(\frac{[H^+]}{K_{a1}} + 1 + \frac{K_{a2}}{[H^+]} \right)} \quad (2)$$

low pH, intermediate pH, and high pH, respectively. Best-fit parameters are collected in Table S4.

A preliminary interpretation of the data is that K_A^{acid} represents the binding of the imidazolium ion to *BjFixLH*, with a value of $39 \pm 11 \text{ M}^{-1}$, K_A^{neut} represents the binding of imidazole to *BjFixLH* with a value of $(1.6 \pm 0.3) \times 10^3 \text{ M}^{-1}$, and K_A^{base} represents binding of imidazole to the alkaline, hydroxyl-ligated form of *BjFixLH*. K_A^{base} is equal to zero with an estimated error of $\pm 57 \text{ M}^{-1}$. This mechanism is not completely satisfactory since the best-fit values for the two ionizations are 8.0 ± 0.1 and 10.0 ± 0.2 , significantly different from the independently determined values of 7.04 ± 0.02 [29] and 9.64 ± 0.05 , Fig. 2, for the ligand and protein ionizations, respectively.

3.4. Kinetics of cyanide binding to *BjFixLH* and *SmFixLH*

The rate of cyanide binding to the heme domains of *FixL* was investigated under pseudo first-order condition using stopped-flow techniques between pH 5 and 11.5. The reaction is monophasic with the observed rate constant linearly dependent upon the cyanide concentration between pH 5 and 9.5, Fig. S7. The data are consistent

with reversible complex formation, Eq. (3). Under pseudo-first order conditions, where $[L] \gg [P]$, the observed rate constant, k_{obs} , will be.



given by Eq. (4). Values of the association rate constant, k_a , and the dissociation rate constant, k_d ,

$$k_{obs} = k_a[L] + k_d \quad (4)$$

can be determined from the slope and intercept of plots of k_{obs} versus ligand concentration, Fig. S7. At pH 10 and above, the plots of k_{obs} versus ligand concentration have a slight upward curvature, Fig. S8, and k_{obs} was fit to a quadratic function of the ligand concentration. Values of k_a were determined from the limiting slope of the quadratic plots at low ligand concentration.

While the values of k_a determined from the slope of plots such as those shown in Figs. S7 and S8 were very precise, with a standard deviation of about 9%, the k_d values determined from the intercepts are small and highly variable. The intercepts are very close to the origin and some of the intercept values were negative. It was decided to evaluate the dissociation rate constant by calculating k_d from the relationship, $k_d = k_a K_D$. Values of k_a and k_d , are given in Tables S1 and S2 for *BjFixLH* and *SmFixLH*, respectively. Plots of the logarithm of k_a and k_d as functions of the pH are shown in Fig. 6 for *BjFixLH* and in Fig. S9 for *SmFixLH*.

A previous study of cyanide binding to two truncated versions of *SmFixL* reported k_a values of 27 and $31 \text{ M}^{-1} \text{ s}^{-1}$ for the heme domain (*RmFixLH*) and for the combined heme/kinase domains (*RmFixLT*) at pH 8, 20 mM Tris-HCl buffer [21]. In this study, we find a k_a value of $62 \pm 5 \text{ M}^{-1} \text{ s}^{-1}$ for our preparation of *SmFixLH* at pH 8.0 in a 0.100 M

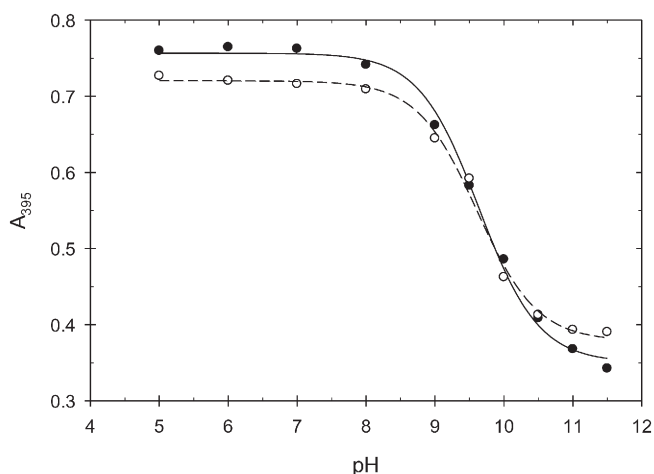


Fig. 2. Plot of the absorbance at 395 nm as a function of pH for *BjFixLH* (solid circles) and *SmFixLH* (open circles).

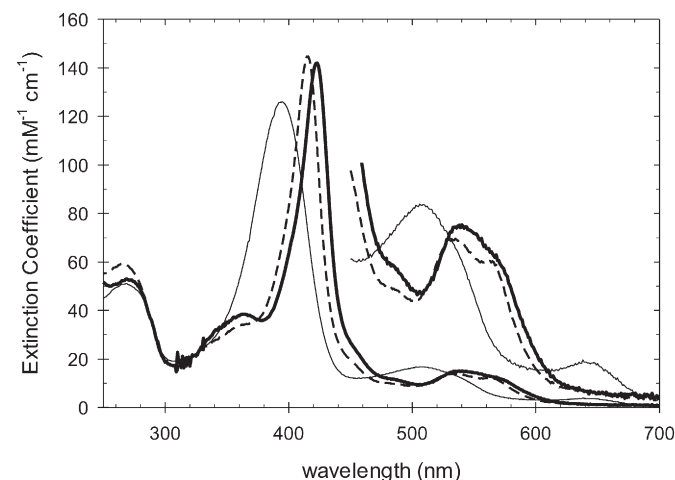


Fig. 3. The absorption spectra of penta-coordinate met-*BjFixLH* (thin solid line), cyano-*BjFixLH* (thick solid line), and the imidazole complex of *BjFixLH* (dashed line) at pH 7.0.

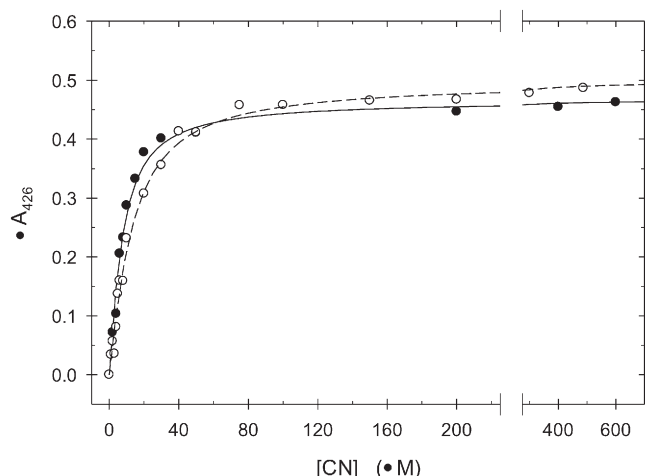


Fig. 4. Titration of 4.78 μM *BjFixLH* (solid circles) and 5.85 μM *SmFixLH* (open circles) with cyanide at pH 7.0.

ionic strength potassium phosphate buffer, Table S2. The factor of 2 differences between the two studies may be due to differences in ionic strength. At pH 8.0, a 20 mM Tris–HCl buffer has an ionic strength of ~ 0.011 M compared to 0.10 M in our study. We also observe that the heme domain of *BjFixLH* binds cyanide about 65% faster than *SmFixLH* at pH 8.0, with an observed rate constant of $102 \pm 1 \text{ M}^{-1} \text{ s}^{-1}$, Table S1.

3.5. pH dependence of the association and dissociation rate constants for the *BjFixLH* and *SmFixLH* cyanide complexes

The value of k_a is a bell-shaped function of the pH with a maximum near pH 9.5 indicating that at least two ionizable groups in the reactants affect the rate of cyanide binding, Figs. 6 and S9. The most obvious ionizations are those of the ligand, HCN, with a $\text{p}K_a$ of 9.04 at 0.10 M ionic strength [30], and the alkaline transition in the heme domains of the FixLs, Fig. 2, with $\text{p}K_a$ s of 9.64 ± 0.05 and 9.61 ± 0.05 for *BjFixLH* and *SmFixLH*, respectively. The data in Figs. 6 and S9 were initially fit to an empirical equation involving two ionizable groups. The best-fit values for the two $\text{p}K_a$ s were 8.53 ± 0.07 and 10.03 ± 0.13 for the *BjFixLH* data and 8.55 ± 0.12 and 9.94 ± 0.16 for the *SmFixLH* data. The fitted $\text{p}K_a$ values do not correspond to either the $\text{p}K_a$ s for the alkaline transition in the heme domains or the $\text{p}K_a$ for ionization of HCN.

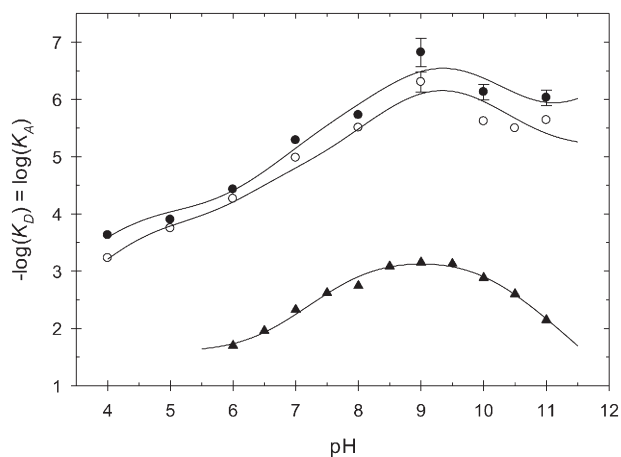


Fig. 5. pH dependence of the equilibrium constants for cyanide binding to *BjFixLH* (solid circles), cyanide binding to *SmFixLH* (open circles), and imidazole binding to *BjFixLH* (solid triangles).

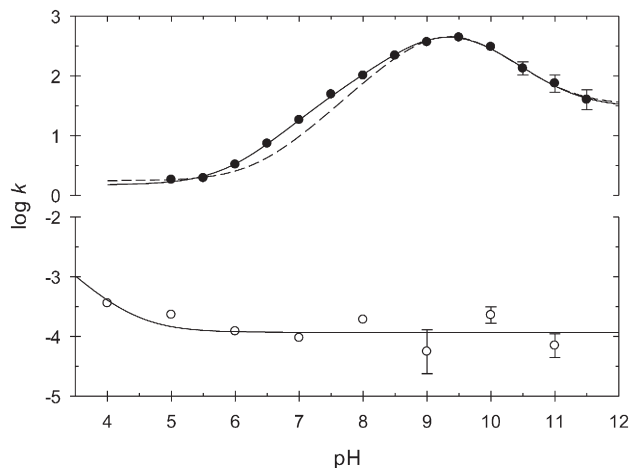


Fig. 6. pH dependence of the association (solid circles) and dissociation (open circles) rate constants for cyanide binding to *BjFixLH*.

A more detailed analysis of the pH dependence of k_a suggests that a second ionizable group in the heme domains affects cyanide binding. If we fit the k_a data by fixing the $\text{p}K_a$ values to 9.04 for the ligand and either 9.64 for *BjFixLH* or 9.61 for *SmFixLH*, and then fitting the peak position and the values of k_a at the pH extremes we generate the dashed lines shown in Figs. 6 and S9. The fit is excellent above pH 8.5 but underestimates the value of k_a between pH 6 and 8.5. We propose that a second ionizable group in the heme domain affects binding of cyanide below pH 8.5 and include the second group in a mechanism to be discussed below.

The dissociation rate constant is essentially independent of pH between 5 and 11 but appears to increase slightly at pH 4, Figs. 6 and S9. The average value of k_d between pH 5 and 11 is $(1.4 \pm 0.7) \times 10^{-4} \text{ s}^{-1}$ for *BjFixLH* and $(2.1 \pm 1.0) \times 10^{-4} \text{ s}^{-1}$ for *SmFixLH*.

3.6. Kinetics of imidazole binding to *BjFixLH*

Kinetic studies of the binding of imidazole to *BjFixLH* were carried out under pseudo-first order conditions using a stopped-flow instrument. The reaction was monitored at 418 nm after 1:1 mixing of the protein and imidazole solutions. The reaction was monophasic and fit to a single exponential equation to obtain the observed rate constants, k_{obs} . The reaction was studied as a function of imidazole concentration over the pH range 5.0 to 11.0. A typical plot of the concentration dependence of k_{obs} is shown in Fig. S10.

The rate of imidazole binding saturates at high imidazole concentrations and was fit to the empirical equation shown in Eq. (5). The interpretation of the three parameters, P1, P2, and P3

$$k_{obs} = \frac{P1[L] + P2}{P3[L] + 1} \quad (5)$$

depends upon the mechanism of ligand binding and will be discussed below. P1 and P2 can be thought of as apparent association and dissociation rate constants, respectively, and the ratio P1/P3 gives the maximum value of k_{obs} at very high ligand concentrations. Values of P1, P2, and P3 were determined between pH 5 and 11 and are collected in Table S3.

The values of all three parameters are pH dependent. The logarithm of each of the three parameters is plotted in Fig. 7. Each of the parameters appears to depend upon two ionizations over the pH range investigated and each was fit to an equation similar to Eq. (2). The best-fit values for the $\text{p}K_a$ s and the low, intermediate, and high pH limits for each of the three kinetic parameters are collected in Table S5.

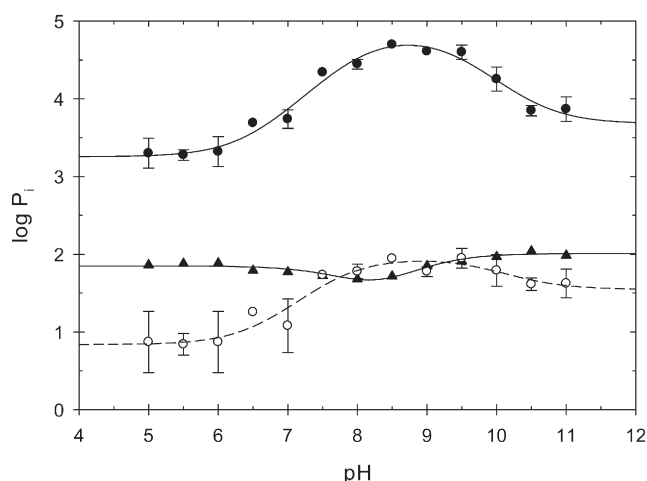


Fig. 7. pH dependence of P1 (solid circles), P2 (solid triangles), and P3 (open circles) for the binding of imidazole to *BjFixLH*.

3.7. Kinetics of imidazole binding to *SmFixLH*

Imidazole binding to *SmFixLH* is very similar to that of *BjFixLH*. Values of the three kinetic parameters P1, P2, and P3 were determined over the pH range 5 to 11 and are collected in Table S6. Plots of P1, P2, and P3 as a function of pH are shown in Fig. S11. Each of the parameters were fit to an empirical equation similar to that of Eq. (2) and best-fit values for the pK_a s and the low, intermediate, and high pH limits for each of the parameters are collected in Table S7.

3.8. Kinetics of imidazole binding to *SmFixLH*(Y197F)

Tyrosine 197 ionizes in a similar pH region as that for formation of the alkaline form of *SmFixLH* and may influence ligand binding at high pH [31]. The rate of imidazole binding to the Y197F mutant of *SmFixLH* was determined between pH 5 and 11 and is similar to that for imidazole binding to *SmFixLH*. Values of the three kinetic parameters P1, P2, and P3 are collected in Table S8. Plots of P1, P2, and P3 for the imidazole-*SmFixLH*(Y197F) reaction as a function of pH are shown in Fig. S12. Each of the parameters were fit to an empirical equation similar to that of Eq. (2) and best-fit values for the pK_a s and the low, intermediate, and high pH limits for each of the parameters are collected in Table S9.

3.9. Kinetics of 4-nitroimidazole binding to *SmFixLH*

The nitro group in 4-nitroimidazole significantly increases the acidity of the imidazole group. The pK_a for ionization of the 4-nitroimidazolium ion is less than 0 while the pK_a for the 4-nitroimidazole to 4-nitroimidazolate ionization is 8.96 ± 0.09 at 0.10 M ionic strength [32]. As a consequence, the 4-nitroimidazole ligand will be primarily neutral between pH 5 and 9 in this study and predominantly negatively charged between pH 9 and 11. 4-Nitroimidazole is relatively insoluble in water and the ligand binding studies were limited to 4-nitroimidazole concentrations of less than 6 mM after 1:1 mixing in the stopped-flow instrument. Under these conditions the observed rate constant for 4-nitroimidazole binding to *SmFixLH* is linearly dependent upon the ligand concentration and only the parameters P1 and P2 can be determined. Values of P1 and P2 are collected in Table S10. Plots of the logarithm of P1 and P2 as a function of pH are shown in Fig. S13.

The logarithm of P1 has a bell-shaped dependence on pH indicating that it is influenced by a minimum of two ionizable groups. P1 was fit to an empirical equation analogous to Eq. (2) and the best-fit values for the kinetic parameters are collected in Table S11. Interestingly, in the

absence of constraints, the best-fit value of pK_{a1} is larger than the value of pK_{a2} and non-linear least-squares regression gives very high estimated errors for the kinetic parameters. If pK_{a1} is constrained to be less than or equal to pK_{a2} , the two values converge of a value of 9.2 ± 1.0 and the estimated errors of the fitted parameters are reduced significantly.

The value of P2 is independent of pH between pH 8 and 11, with an average value of $1.1 \pm 0.1 \text{ s}^{-1}$ and increases by about a factor of 3 as the pH is lowered from 8 to 7.

4. Discussion

4.1. Mechanism of cyanide binding to *BjFixLH* and *SmFixLH*

The binding of cyanide to *FixLH* appears to be a simple, monophasic ligand binding reaction characterized by association and dissociation rate constants consistent with the equilibrium dissociation constants, Eq. (3). Cyanide is small enough to diffuse into the distal heme pocket of *FixL*, bind to the heme iron and convert the heme from a five-coordinate high-spin species to a six-coordinate low-spin species. Conformational adjustments in the heme domain associated with cyanide binding occur on a time scale much faster than the rate of ligand binding. Under the conditions of our experiments, the maximum value of k_{obs} for cyanide binding is less than 10 s^{-1} , Figs. S7 and S8.

The pH dependence of the association rate constant indicate a minimum of two ionizable groups within the heme domain of *FixL* influence cyanide binding to the heme domain of *FixL* (Section 3.5). A minimal mechanism to explain the pH dependence of cyanide binding to the heme domain of *FixL* is shown in Scheme 1.

Scheme 1 postulates that three different protonated forms of the protein affect cyanide binding, HP, P, and POH, and these forms are related by pK_{p1} and pK_{p2} . The group with pK_{p1} is attributed to the propionic acid group at heme position 6, HP6, (for reasons to be discussed in Section 4.5) while pK_{p2} is due to formation of the hydroxy-*FixLH*, Figs. 1 and 2. Scheme 1 allows for diffusion of both HCN and the cyanide anion (CN^-) into the distal heme pocket and binding to the heme iron in each of the three different protonated forms of the protein. When HCN binds to either HP or P, the ligand proton is released into solution. When HCN binds to POH, the HCN proton is transferred to the departing OH^- and released as water. When CN^- binds to POH, there is anion exchange and the hydroxide ion is released into solution.

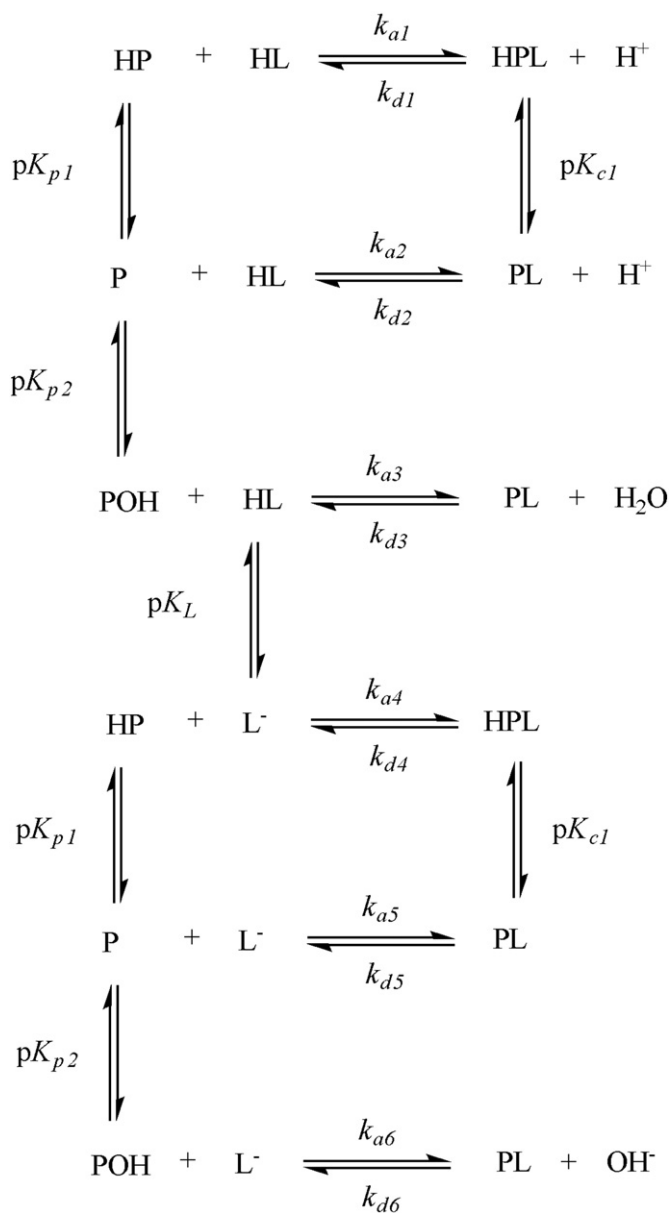
4.2. pH dependence of the cyanide association rate constant

The pH dependence of k_a , derived from Scheme 1 is given by Eq. (6). In Eq. (6), pK_{p1} and pK_{p2} are the pK_a values of two groups in the heme domain that affect cyanide binding and pK_L is

$$k_a = \frac{k_{a1} \frac{[\text{H}^+]^2}{K_L K_{p1}} + \left(k_{a2} \frac{K_{p1}}{K_L} + k_{a4} \right) \frac{[\text{H}^+]}{K_{p1}} + \left(k_{a3} \frac{K_{p2}}{K_L} + k_{a5} \right) + k_{a6} \frac{K_{p2}}{[\text{H}^+]}}{\left(\frac{[\text{H}^+]}{K_{p1}} + 1 + \frac{K_{p2}}{[\text{H}^+]} \right) \left(1 + \frac{[\text{H}^+]}{K_L} \right)} \quad (6)$$

the pK_a for the ligand, HCN. In fitting the data, we fixed pK_L at 9.04 and pK_{p2} at 9.64 and 9.61 for the alkaline transitions of *BjFixLH* and *SmFixLH*, respectively. There are five adjustable parameters and these are defined in Table 2 along with the best-fit values for both the *BjFixLH* and *SmFixLH* data. The solid lines through the k_a data in Figs. 6 and S9 were calculated using Eq. (6). The fit is excellent and Scheme 1 is sufficient to account for the pH dependence of cyanide binding to the heme domains of *FixL*.

Allowing both HCN and CN^- to bind to *FixLH* in Scheme 1 perhaps obscures the general picture of cyanide binding. In the Supplementary Data (Section 4.2) we discuss the analysis of the pH dependence of



Scheme 1. Mechanism for cyanide binding to FixLH.

the association rate constant in detail. Here we present a simplified overview of cyanide binding to FixLH. The maximum rate of cyanide binding to *BjFixLH* occurs at pH 9.5 with an observed rate constant, k_a ,

Table 2
Kinetic parameters for cyanide binding to *BjFixLH* and *SmFixLH*.^a

Parameter	<i>BjFixLH</i>	<i>SmFixLH</i>
k_{a1} ($\text{M}^{-1} \text{s}^{-1}$)	1.5 ± 0.1	1.5 ± 0.2
$(k_{a2} \frac{k_{p1}}{K_1} + k_{a4})$ ($\text{M}^{-1} \text{s}^{-1}$)	$(2.1 \pm 0.8) 10^3$	$(2.6 \pm 0.8) 10^3$
$(k_{a3} \frac{k_{p2}}{K_1} + k_{a5})$ ($\text{M}^{-1} \text{s}^{-1}$)	960 ± 40	640 ± 30
k_{a6} ($\text{M}^{-1} \text{s}^{-1}$)	30 ± 3	0.4 ± 0.9
$\text{p}K_{p1}$	7.6 ± 0.2	6.8 ± 0.2
$\text{p}K_{p2}$	9.64	9.61
$\text{p}K_L$	9.04	9.04
$(\frac{k_{d1}K_{c1} + k_{d4}}{K_{c1}})$ ($\text{M}^{-1} \text{s}^{-1}$)	2.9 ± 2.2	7.9 ± 4.5
$(k_{d3} + k_{d5})$ (s^{-1})	$(1.2 \pm 0.3) \times 10^{-4}$	$(1.7 \pm 0.3) \times 10^{-4}$
$\text{p}K_{c1}$	<5	<5

^a Parameters defined in Scheme 1 of the text.

^b $\text{p}K_L$ and $\text{p}K_{p2}$ were fixed at independently determined values.

of $443 \pm 8 \text{ M}^{-1} \text{ s}^{-1}$ (Table S1). The maximum observed rate is primarily due to the binding of CN^- to protein form P in Scheme 1, the k_{a5} pathway, which is the dominant pathway for cyanide binding between pH 8 and 11. Above pH 11, the k_{a6} pathway in Scheme 1, CN^- binding to POH, makes a significant contribution to the observed rate constant, k_a . In the neutral pH region, between about pH 6 to 8, the dominant pathway is the binding of CN^- to HP (k_{a4}). The binding of HCN only becomes significant below pH 6, where the concentration of CN^- is less than 0.1% of the total cyanide concentration in solution. The binding of HCN to HP, with a rate constant k_{a1} of $1.5 \text{ M}^{-1} \text{ s}^{-1}$ is responsible for the low pH limit of the observed association rate constant. The cyanide anion is the reactive form of the ligand and dominates the rate of binding to FixLH over the pH region 6 to 11.5.

The pH dependence of k_a for *SmFixLH* is very similar to that of *BjFixLH*. The observed rate constant is somewhat lower with a maximum value $252 \text{ M}^{-1} \text{ s}^{-1}$ between pH 9 and 9.5 (Table S2). The only major difference in the fitting parameters between *SmFixLH* and *BjFixLH* is for k_{a6} , Table 2. The fitted value of k_{a6} is $30 \pm 3 \text{ M}^{-1} \text{ s}^{-1}$ for *BjFixLH* and $0.4 \pm 0.9 \text{ M}^{-1} \text{ s}^{-1}$ for *SmFixLH*. Binding of cyanide to the alkaline form of *SmFixLH* makes no significant contribution to the observed association rate constant up to pH 11.5, the limit of our study. On the other hand, the value of k_a for *BjFixLH* appears to reach a finite asymptote at high pH, Fig. 6, indicating that cyanide does bind to the alkaline form of *BjFixLH*. Cyanide binding to the hexa-coordinate alkaline form of *BjFixLH* ($k_{a6} = 30 \text{ M}^{-1} \text{ s}^{-1}$) is more than 30-fold slower than binding to the five-coordinate, neutral form of *BjFixLH* ($k_{a5} = 960 \text{ M}^{-1} \text{ s}^{-1}$).

4.3. pH dependence of cyanide dissociation rate constant

The dissociation rate constant is essentially independent of pH with a small increase at pH 4, Figs. 6 and S9. There are only two forms of the complex in Scheme 1, HPL and PL. The two species are related by the acid dissociation constant, $\text{p}K_{c1}$. Scheme 1 allows for perturbation of the $\text{p}K_a$ of the acidic group in the cyanide complex ($\text{p}K_{c1}$) relative to its value in the ligand-free protein ($\text{p}K_{p1}$). For completeness, Scheme 1 includes the proton-assisted ligand dissociation pathways, with rate constants k_{d1} and k_{d2} , at low pH and the hydroxide ion-assisted pathway, k_{d6} , at high pH. The pH dependence of k_d derived from Scheme 1 is given by Eq. (7). All of the

$$k_d = \frac{k_{d1} \frac{[\text{H}^+]^2}{K_{c1}} + (k_{d2}K_{c1} + k_{d4}) \frac{[\text{H}^+]}{K_{c1}} + (k_{d3} + k_{d5}) + k_{d6}[\text{OH}^-]}{\left(\frac{[\text{H}^+]}{K_{c1}} + 1\right)} \quad (7)$$

parameters included in Eq. (7) are not required to fit the data. First, there is no indication that the values of k_d increase with increasing hydroxide ion concentration as suggested by the $k_{d6}[\text{OH}^-]$ term in the numerator and this term can be eliminated. The dissociation rate is essentially constant between pH 5 and 11 indicating that the $(k_{d3} + k_{d5})$ term is dominant over most of the pH range. Finally, the small increase in k_d at pH 4 suggests that the second term in the numerator of Eq. (7) is just beginning to make a contribution to the dissociation rate and that the first term in the numerator is negligible. The data suggest that we have not attained low enough pH to significantly protonate PL, which means that the $[\text{H}^+] / K_{c1}$ term in the denominator is negligible and that $\text{p}K_{c1} < 5$. Using these considerations, Eq. (7) simplifies to Eq. (8).

$$k_d = \left(\frac{k_{d2}K_{c1} + k_{d4}}{K_{c1}}\right) [\text{H}^+] + (k_{d3} + k_{d5}) \quad (8)$$

The dissociation rate constants were fit to Eq. (8) using non-linear least squares regression and the best-fit values for the parameters are included in Table 2. The lines through the data in Figs. 6 and S9 were calculated using Eq. (8). In the complex, $\text{p}K_{c1}$ is less than 5, which means

that PL is the dominant species over the entire pH range between 5 and 11. Cyanide dissociates from PL with a rate $(k_{d3} + k_{d5}) = (1.2 \pm 0.3) \times 10^{-4}$ and $(1.7 \pm 0.3) \times 10^{-4} \text{ s}^{-1}$ for cyano-BjFixLH and cyano-SmFixLH, respectively. The dissociation rate agrees quite well with two previous values determined at pH 8, $1.0 \times 10^{-4} \text{ s}^{-1}$ for RmFixLH and $1.5 \times 10^{-4} \text{ s}^{-1}$ for RmFixLT [21].

4.4. pH dependence of K_D for the cyanide complexes of FixLH

The pH dependence of K_D , Fig. 5, is given by the ratio k_d/k_a as described by Eqs. (6) and (8). The solid lines for the BjFixLH and SmFixLH data in Fig. 5 were calculated from the ratio of Eqs. (8) to (6) and the parameter values listed in Table 2. The value of K_D determined from the kinetic constants is essentially identical to that determined from the static equilibrium studies over the entire pH range of this study. This observation supports the conclusion that cyanide binding to FixLH is a simple ligand association reaction and that any conformational changes associated with ligand binding influence both the kinetic and equilibrium properties in an identical fashion. The behavior of the cyanide-FixLH system is in contrast with that of imidazole binding to FixLH, where it is found that the K_D values calculated from the kinetic parameters do not agree with the static determination of K_D above 9, Section 4.6.

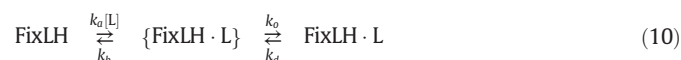
4.5. Identification of acidic group influencing cyanide binding to BjFixLH and SmFixLH

One of the intriguing questions raised by this study is the identity of the acidic group affecting the rate and affinity of cyanide binding to the heme domains of FixL. According to our interpretation of the data, the acidic group has apparent pK_a values of 7.6 in BjFixLH and <5 in the cyanide complex. We have used the crystal structures of BjFixLH and its cyano complex to determine if any of the acidic groups within the protein undergo significant environmental changes upon cyanide binding that could account for the shift in pK_a [10,13]. After consideration of the six acidic groups within 10 Å of the heme iron in the ligand-free state: heme propionic acids 6 (HP6) and 7 (HP7), Asp-196, Asp-201, Tyr-203, and Arg-220, we conclude that the ionizable group with pK_a 7.6 in BjFixLH is most likely HP6. (See Section 4.5 of the Supplementary Data for details.)

4.6. Mechanism of imidazole binding to FixLH

Another intriguing question addressed by this study concerns the early observation that the imidazole binding to FixLH was about two orders of magnitude faster than binding to metMb, suggesting initially that the FixLH distal heme pocket was freely accessible to large ligands [21,23]. However, the crystal structure of BjFixLH shows that the distal heme pocket in BjFixLH is quite crowded and cannot accommodate a bulky ligand such as imidazole without significant rearrangement of the distal pocket residues [10,11,13]. A comparison of the crystal structures of BjFixLH and of the BjFixLH-imidazole complex shows large movements of Ile-215 and Ile-238 to accommodate the bound imidazole.

Two plausible mechanisms for imidazole binding to FixLH that incorporate saturation of the binding rate at high imidazole concentrations, are shown in Eqs. (9) and (10). In the



“conformational gating” mechanism shown in Eq. (9), the heme domain exists as an equilibrium mixture of closed (FixLH) and open (FixLH*)

conformations, with the closed conformation predominating in the absence of ligand. The heme pocket opens with a rate constant k_o and closes in a back reaction with rate constant k_b , where $k_b \gg k_o$. Imidazole binds to the heme iron when the protein is in the open conformation with an association rate constant k_a and dissociates from the heme iron with a rate constant k_d . The conformational equilibrium lies very far to the left and the equilibrium concentration of FixLH* is very small and can be considered to be in a steady-state throughout the ligand binding reaction. Using the steady-state assumption, the concentration dependence of the observed rate constants is given by Eq. (5) where $P1 = k_a k_o / k_b$, $P2 = k_d$, and $P3 = k_a / k_b$.

An alternative mechanism is the “encounter complex” mechanism shown in Eq. (10). Initially, imidazole binds to the closed conformation of FixLH to form an encounter complex, {FixLH·L}, in which the ligand is associated with the protein but not bound to the heme iron. Conformational fluctuations within the encounter complex cause opening of the distal heme pocket with a rate constant k_o , allowing the ligand to move into the heme pocket and bind to the heme iron. The rate of dissociation of the ligand from the heme iron is designated k_d , but this leads to reformation of the encounter complex rather than dissociation into solution. The rate of ligand dissociation from the encounter complex into solution is designated k_b . Assuming that the encounter complex is in a steady-state during the ligand binding reaction, the observed rate constant is again given by Eq. (5) but the definitions of the parameters are altered compared to the conformational gating mechanism. For the encounter complex mechanism, Eq. (10), $P1 = k_a k_o / (k_b + k_o)$, $P2 = k_d k_b / (k_b + k_o)$, and $P3 = k_a / (k_b + k_o)$.

The two mechanisms for imidazole binding to FixLH shown in Eqs. (9) and (10) provide a rationale for the larger apparent association rate constant for imidazole binding to FixLH compared to imidazole binding to metMb. In both mechanisms, the limiting rate at low imidazole concentrations is not the association rate constant for binding of imidazole to the stable, sterically-crowded heme pocket of FixLH, but an apparent rate constant. For the conformational gating mechanism, the apparent rate constant is for imidazole binding to an “open” form of the heme pocket, multiplied by the equilibrium constant between the open and closed conformations of FixLH, k_o/k_b . The ratio k_o/k_b has to be significantly smaller than one, and the actual association rate constant for binding to the open form of FixLH must be significantly larger than the observed values of $P1$ for BjFixLH and SmFixLH, which vary between $1.9 \times 10^3 \text{ M}^{-1} \text{ s}^{-1}$ to $7.0 \times 10^4 \text{ M}^{-1} \text{ s}^{-1}$, Tables S3 and S5. This is actually quite reasonable. Ligand binding to the heme in metMb is blocked by the distal histidine and access to the heme requires the movement of the distal histidine to open the heme pocket. This movement is fast enough in metMb so that saturation of ligand binding rates is not typically observed. Mansy et al. [23] have shown that replacing the distal histidine in metMb by an alanine residue increase the imidazole association rate constant almost four orders of magnitude from $1.6 \times 10^2 \text{ M}^{-1} \text{ s}^{-1}$ to $1.0 \times 10^6 \text{ M}^{-1} \text{ s}^{-1}$. Rate constants of the order of $10^6 \text{ M}^{-1} \text{ s}^{-1}$ or larger could well be expected for a completely open, uninhibited conformation of FixLH.

In the encounter complex mechanism, the apparent association rate constant, $P1$, is for formation of the encounter complex, modified by the rates of heme pocket opening and dissociation of the imidazole from the encounter complex, $k_a k_o / (k_b + k_o)$. Formation of encounter complexes can be diffusion controlled and the value of k_a could be as large as $10^9 \text{ M}^{-1} \text{ s}^{-1}$. The ratio of $k_o / (k_b + k_o)$ is necessarily less than unity, decreasing the apparent association rate constant to the values shown by $P1$ in Tables S3 and S5 for BjFixLH and SmFixLH, respectively.

For reasons to be discussed in Section 4.9, the encounter complex mechanism provides a simpler interpretation for the pH dependence of the kinetic parameters than the conformational gating mechanism. Because of this, we analyze the details of imidazole binding to FixLH using the encounter complex mechanism. Additional comments on the conformational gating mechanism can be found in Section 4.6 of the Supplementary Data.

In terms of the encounter complex mechanism, P1 is an apparent association rate constant and provides a lower-limit to the true association rate constant for encounter complex formation. P2 is an apparent dissociation rate, again giving a lower limit to the true rate of imidazole dissociation from the heme. P3 has the units of an equilibrium association constant and determines the curvature in the plots of k_{obs} as a function of the imidazole concentration, Fig. S10.

Two combinations of the kinetic parameters provide useful information. $P1/P2 = k_a k_o / k_d k_b = K_A$, where K_A is the equilibrium association constant for binding of imidazole to FixLH. Also, the ratio $P1/P3 = k_o$ gives the rate of heme pocket opening. The latter is an important parameter providing information on the dynamics of the conformational changes in FixL.

A comparison of the value of P1/P2 with that of the independently determined value of K_A for BjFixLH is shown in Fig. S14 of the Supplementary Data. There is good agreement between the values of P1/P2 and K_A below pH 9, but K_A is significantly larger than P1/P2 at pH ≥ 9 . This indicates that the encounter complex mechanism is consistent with imidazole binding to the acidic form of BjFixLH, but is inadequate to explain imidazole binding above pH 9 where the alkaline form of BjFixLH is dominant in solution. We postulate that the initial imidazole-FixLH complex observed at the end of the reaction detected with the stopped-flow instrument is stabilized by a second, slower reaction above pH 9, which may occur over the period of hours. K_A was determined from overnight incubations of FixLH and imidazole.

The ratio P1/P3 gives the rate of heme pocket opening, k_o . The rate of heme pocket opening limits the rate of imidazole binding to the heme in FixLH giving the hyperbolic plots of k_{obs} as a function of the imidazole concentration, Fig. S10. Values of P1/P3 are plotted as a function of pH in Fig. 8 for BjFixLH, SmFixLH, and SmFixLH(Y197F). Experimental values of k_o vary between a maximum of 1450 s^{-1} for the SmFixLH(Y197F) reaction at pH 5 to a minimum value 100 s^{-1} for the SmFixLH reaction at pH 11. The crystallographic data suggest that opening of the heme pocket to allow imidazole binding involves significant movement of Ile-215 and Arg-220 [10,11]. Gong et al. find that in order to accommodate a heme-bound imidazole, the sidechain of Ile-238 rotates away from the heme iron but that the majority of the space needed to accommodate imidazole is due to a 2.2 Å movement of the Ile-215 side chain, which is associated with the shift of the FG loop away from the heme pocket [11]. In addition Arg-220 breaks its hydrogen bond with HP7 and rotates toward the surface of FixLH. The large scale movements of Ile-215 and Arg-220 could be associated with rates in the 100 to 1450 s^{-1} range as observed for k_o .

4.7. pH dependence of the kinetic parameters for imidazole binding to FixLH

The pH dependence of the three kinetic parameters P1, P2, and P3 can be explained by Scheme 2, an expanded form of the encounter complex mechanism that includes the involvement of different protonated forms of the protein and ligand. Scheme 2 is also an expanded version of Scheme 1, the mechanism used to interpret the pH dependence of cyanide binding to FixLH.

The initial reaction manifold is the same in Schemes 1 and 2. However, the initial ligand binding steps in Scheme 2 form an encounter complex while in Scheme 1, the initial ligand binding steps give the final product. Scheme 2 includes the additional reaction steps necessary for conversion of the encounter complex into the stable complex, the steps that are responsible for limiting the observed rate of imidazole binding to FixLH.

The empirical fits of P1, P2, and P3 to Eq. (2) indicate that two ionizations influence the kinetics of imidazole binding to BjFixLH, Table S5. The more acidic group has an apparent pK_a in the range of 7 to 8, while the second group has an apparent pK_a in the range of 9.2 to 10. These values are consistent with cyanide binding to BjFixLH, which is influenced by two protein ionizations with pK_a values of 7.6 ± 0.2 and 9.64 ± 0.05 , Table 2. In the case of cyanide binding, the more acidic

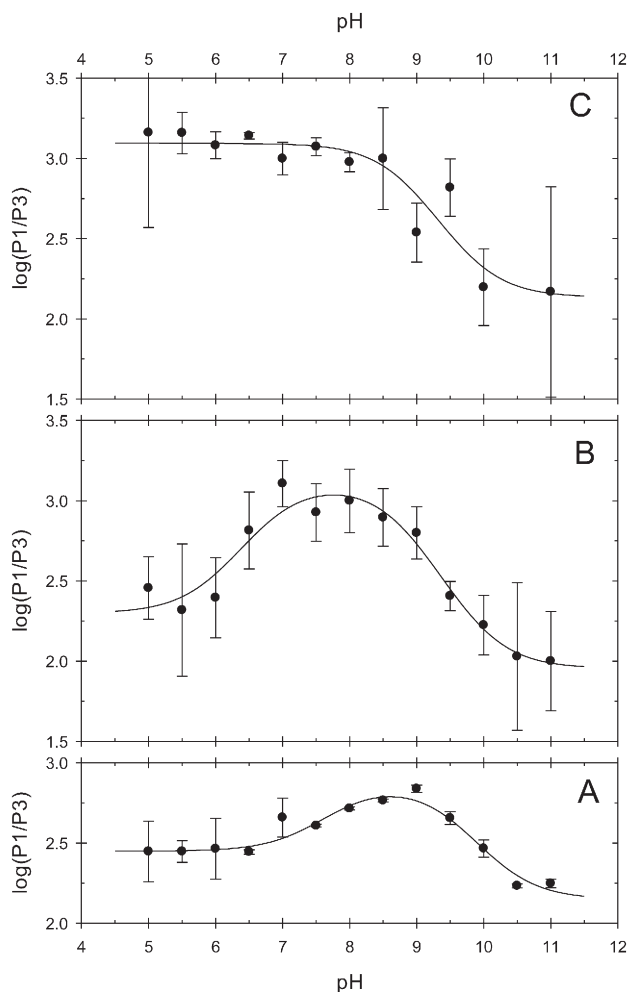


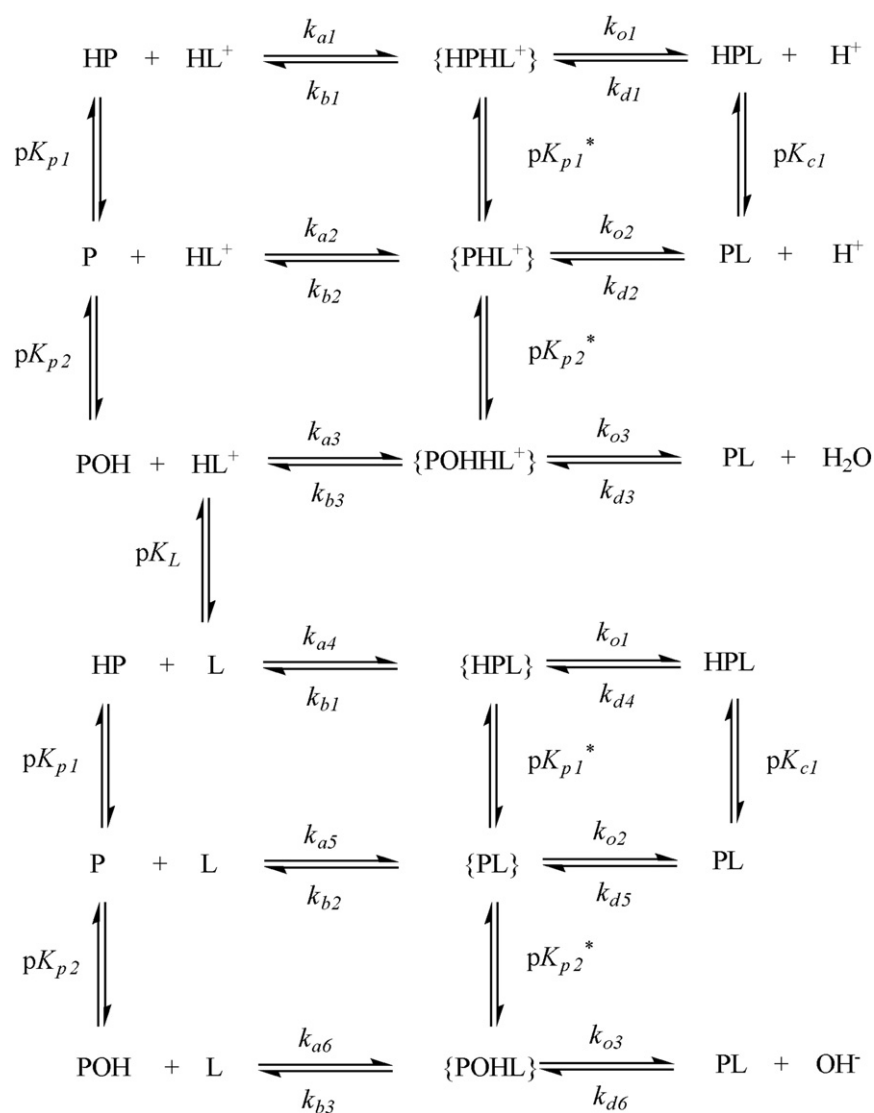
Fig. 8. Plots of the logarithm of $P1/P3 = k_o$ as a function of pH for imidazole binding to FixLH. Panel A. BjFixLH. Panel B. SmFixLH. Panel C. SmFixLH(Y197F).

group is attributed to HP6 and the more alkaline transition is due to formation of the alkaline, hydroxy-ligated BjFixLH (Section 4.5).

Scheme 2 allows binding of both imidazole (L) and the imidazolium ion (HL^+) to the protein to form the encounter complex giving rise to six different protonated forms of the encounter complex. Scheme 2 allows for the perturbation of the protein pK_a values in the encounter complex, and designates their encounter complex values as pK_{p1}^* and pK_{p2}^* . While it is possible that binding of the ligand to the protein could alter the apparent pK_a of the ligand, this is explicitly excluded from the mechanism. Any perturbation of pK_L upon encounter complex formation will contribute to the observed values of pK_{p1}^* and pK_{p2}^* . As will be seen later the perturbation of the apparent pK_a values for the protein ionizations upon encounter complex formation are quite small. The pH dependencies of k_a , k_d , k_o , and k_b are given by Eqs. (11)–(14), below

$$k_a = \frac{k_{a1} \frac{[H^+]^2}{K_L K_{p1}} + \left(k_{a2} \frac{K_{p1}}{K_L} + k_{a4} \right) \frac{[H^+]}{K_{p1}} + \left(k_{a3} \frac{K_{p2}}{K_L} + k_{a5} \right) + k_{a6} \frac{K_{p2}}{[H^+]}}{\left(\frac{[H^+]}{K_{p1}} + 1 + \frac{K_{p2}}{[H^+]} \right) \left(\frac{[H^+]}{K_L} + 1 \right)} \quad (11)$$

$$k_b = \frac{k_{b1} \frac{[H^+]}{K_{p1}} + k_{b2} + k_{b3} \frac{K_{p2}}{[H^+]}}{\left(\frac{[H^+]}{K_{p1}} + 1 + \frac{K_{p2}}{[H^+]} \right)} \quad (12)$$



Scheme 2. Mechanism for imidazole binding to FixLH.

$$k_o = \frac{k_{o1} \frac{[H^+]}{K_{p1}^*} + k_{o2} + k_{o3} \frac{K_{p2}^*}{[H^+]}}{\left(\frac{[H^+]}{K_{p1}^*} + 1 + \frac{K_{p2}^*}{[H^+]} \right)} \quad (13)$$

$$k_d = \frac{k_{d1} \frac{[H^+]^2}{K_{c1}} + (k_{d2} K_{c1} + k_{d4}) \frac{[H^+]}{K_{c1}} + (k_{d3} + k_{d5}) + k_{d6} [OH^-]}{\left(\frac{[H^+]}{K_{c1}} + 1 \right)} \quad (14)$$

4.8. pH dependence of the rate of heme pocket opening, $k_o = P1/P3$

The only individual rate constant that can be determined from the experimental kinetic parameters is k_o , which equals P1/P3 in both the conformational gating and encounter complex mechanisms. Fitting P1/P3 to Eq. (13), gives the best-fit values for pK_{p1} , pK_{p2} , k_{o1} , k_{o2} , and k_{o3} that are tabulated in Table 3. The data suggest the pK_a s of the two protein groups do not change (within experimental error) upon formation of the encounter complex, pK_{p1} is 7.6 ± 0.2 in BfFixLH and 7.8 ± 0.4 in the encounter complex while pK_{p2} is 9.64 ± 0.05 in BfFixLH and $9.5 \pm$

0.3 in the encounter complex. The rate of heme pocket opening in the encounter complex varies from 140 s^{-1} at high pH to 730 s^{-1} at intermediate pH. The solid line in Fig. 8 through the P1/P3 data for BfFixLH was calculated according to Eq. (13).

Table 3 also contains the best-fit parameters for SmFixLH and SmFixLH(Y197F). For SmFixLH, pK_{p1} is unperturbed between the ligand free protein and the encounter complex, with a value of 6.8 ± 0.2 in both cases, Table 3, while pK_{p2} goes from 9.61 ± 0.05 in ligand-free SmFixLH, Fig. 2, to 8.8 ± 0.2 in the encounter complex. The more acidic group with pK_{p1} does not affect heme pocket opening in the Y197F mutant of SmFixLH, Table 3, while pK_{p2} in the mutant encounter complex is essentially the same as in the SmFixLH encounter complex, 8.9 ± 0.2 and 8.8 ± 0.2 , respectively. In terms of Scheme 2, the maximum rate of heme pocket opening is given by k_{o2} with values of 730 ± 140 , 1270 ± 290 , and $1240 \pm 160 \text{ s}^{-1}$ for BfFixLH, SmFixLH, and SmFixLH(Y197F), respectively.

4.9. pH dependence of the apparent dissociation rate constant, P2

The pH dependence of P2 is the basis for choosing between the conformational gating and encounter complex mechanisms. The pH dependence of P2 for the three FixLH heme domains under study is not large (Figs. 7, S11, and S12), but it is statistically significant. In the case of the

Table 3
Kinetic parameters derived from Scheme 2 for imidazole binding to FixLH.

Parameter	BjFixLH	SmFixLH	SmFixLH(Y197F)
pK_{p1}^*	7.6 ± 0.2	6.8 ± 0.2	7.2 ± 0.7
pK_{p1}^*	7.8 ± 0.4	6.8 ± 0.3	6.8 ± 0.3
pK_{c1}	<5	<5	<5
pK_{p2}	9.64 ± 0.05	9.61 ± 0.05	8.9 ± 0.3
pK_{p2}^*	9.5 ± 0.3	8.8 ± 0.2	8.9 ± 0.2
pK_L	7.04 ± 0.08	7.04 ± 0.08	7.04 ± 0.08
k_{o1} (s^{-1})	280 ± 20	200 ± 50	1240 ± 160
k_{o2} (s^{-1})	730 ± 140	1270 ± 290	1240 ± 160
k_{o3} (s^{-1})	140 ± 30	90 ± 20	140 ± 40
Contingent parameters	BjFixLH	SmFixLH	SmFixLH(Y197F)
$(k_{d3} + k_{d5})$ (s^{-1}) ^a	[220]	[184]	[326]
k_{b1} (s^{-1}) ^b	510 ± 50	$(2.3 \pm 2.1)10^4$	$(2.0 \pm 1.0)10^3$
k_{b2} (s^{-1}) ^b	300 ± 120	$(6.1 \pm 1.3)10^3$	$(2.8 \pm 1.4)10^3$
k_{b3} (s^{-1}) ^b	$(3.0 \pm 0.7)10^3$	70 ± 28	74 ± 110
k_{a1} ($M^{-1} s^{-1}$) ^b	$(5.6 \pm 1.2)10^3$	$(1.4 \pm 0.4)10^6$	$(7.1 \pm 5.8)10^3$
$(k_{a2} + k_{a4} \frac{K_L}{K_{p1}})$ ($M^{-1} s^{-1}$) ^b	$(5.8 \pm 3.9)10^4$	$(2.9 \pm 6.2)10^5$	$(1.7 \pm 1.2)10^5$
$(k_{a3} + k_{a5} \frac{K_L}{K_{p2}})$ ($M^{-1} s^{-1}$) ^b	$(3.8 \pm 0.7)10^7$	$(1.5 \pm 0.4)10^8$	$(4.0 \pm 0.8)10^7$
k_{a6} ($M^{-1} s^{-1}$) ^b	$(1.5 \pm 0.3)10^5$	$(4.1 \pm 2.4)10^4$	0

^a The value of $(k_{d3} + k_{d5})$ was set equal to twice the maximum value of P2 for each protein.

^b The value of the parameter depends upon the value of $(k_{d3} + k_{d5})$.

BjFixLH imidazole reaction, P2 averages $73 \pm 19 s^{-1}$ over the pH range 5 to 11, varying between $48 \pm 10 s^{-1}$ at pH 8 to $110 \pm 1 s^{-1}$ at pH 10.5, Table S3.

In the conformational gating mechanism, $P2 = k_d$ while in encounter complex mechanism, $P2 = k_d(k_b/(k_b + k_o))$. The empirical fit of the pH dependence of P2 for the BjFixLH imidazole reaction indicates that two ionizations influence this parameter with apparent pK_{a5} of 7.0 ± 0.3 and 9.2 ± 0.2 , Fig. 7 and Table S5. If the conformational gating mechanism were correct, two ionizable groups with pK_{a5} of 7.0 and 9.2 would have to be postulated to affect ligand dissociation from the BjFixLH-imidazole complex. While one of these groups could be the same group as the pK_{p1} group in the ligand-free protein, the complex does not have the equivalent of the alkaline transition in the ligand-free protein, pK_{p2} . A distinct third acidic group in the protein would have to be postulated to accommodate the pH dependence of P2 for the conformational gating mechanism. In the encounter complex mechanism, k_d can be independent of pH and the small pH dependence of P2 can be attributed to the $k_b/(k_b + k_o)$ term. There is no need to postulate the existence of a third acidic group with a pK_a of 9.2 in the imidazole complex. The encounter complex mechanism provides a simpler explanation for the pH dependence of the kinetic parameters for imidazole binding to FixLH and will be used in the following discussion.

P2 is relatively independent of pH for the four imidazole systems investigated in this study, imidazole binding to BjFixLH (Fig. 7), SmFixLH (Fig. S11), and SmFixLH(Y197F) (Fig. S12), as well as for 4-nitroimidazole binding to SmFixLH (Fig. S13). P2 is the only kinetic parameter that depends upon the rate of imidazole dissociation from the heme iron, k_d . For the encounter complex mechanism, $P2 = k_d(k_b/(k_b + k_o))$. Although k_o is dependent upon pH, Fig. 8, the pH dependence of the ratio $k_b/(k_b + k_o)$ will be muted, since both k_b and k_o depend upon the same ionizations in the encounter complex, pK_{p1}^* and pK_{p2}^* . The pH dependence of the ratio $k_b/(k_b + k_o)$ could actually disappear if $k_b \gg k_o$. The preponderance of evidence suggests that the pH dependence of $k_b/(k_b + k_o)$ is small, leading to the conclusion that k_d is also essentially independent of pH. This is consistent with the findings for dissociation of cyanide from FixLH, Fig. 6 and Section 4.3.

Assuming that pK_{c1} is less than 5 in the FixLH-imidazole complex, as it is in the cyanide complex, k_d for both imidazole and cyanide dissociation will be independent of pH over the pH range 5 to 11 and given by $k_d = k_{d3} + k_{d5}$ in terms of the parameters defined in Schemes 1 and 2.

Using these simplifications, the pH dependence of P2 is given by Eq. (15).

$$P2 = \frac{(k_{d3} + k_{d5}) \left(k_{b1} \frac{[H^+]}{K_{p1}^*} + k_{b2} + k_{b3} \frac{K_{p2}^*}{[H^+]} \right)}{\left((k_{b1} + k_{o1}) \frac{[H^+]}{K_{p1}^*} + (k_{b2} + k_{o2}) + (k_{b3} + k_{o3}) \frac{K_{p2}^*}{[H^+]} \right)} \quad (15)$$

Unfortunately, a unique set of parameters cannot be found in fitting the pH dependence of P2 to Eq. (15), even though the values of pK_{p1}^* , pK_{p2}^* , k_{o1} , k_{o2} , and k_{o3} are known from fitting P1/P3 and the problem reduces to finding a set of values for four variables: $k_d = (k_{d3} + k_{d5})$, k_{b1} , k_{b2} , and k_{b3} . The problem is that the values of k_d and k_b are interdependent with changes in k_d compensated by reciprocal changes in k_b .

Since $P2 = k_d(k_b/(k_b + k_o))$ and the ratio $k_b/(k_b + k_o)$ must be less than unity, P2 gives a lower-limit for k_d at each pH. Assuming that k_d is independent of pH as argued above, its minimum value must be at least equal to the largest value of P2 over the pH range 5 to 11. The minimum values of k_d for the BjFixLH, SmFixLH, and SmFixLH(Y197F) imidazole reactions are $110 \pm 1 s^{-1}$ at pH 10.5, $92 \pm 10 s^{-1}$ at pH 5, and $163 \pm 17 s^{-1}$ at pH 7, respectively, Tables S3, S6, and S8. These minimum values for k_d are actually quite large, among the largest reported for dissociation of imidazole from heme protein-imidazole complexes (see Section 4.12) and we suspect that the true rate of imidazole dissociation will not be much larger than these minimum values.

The effect of increasing the value of k_d above its minimum value on the pH dependence of k_b is explored in the Section 4.9 of the Supplementary Data. For reasons discussed in the Supplementary Data, a more realistic set of values for $(k_{d3} + k_{d5})$ is twice the maximum value of P2 for each of the three proteins, i.e., 220, 184, and $326 s^{-1}$ for the BjFixLH, SmFixLH, and SmFixLH(Y197F) imidazole reactions, respectively. These values for $(k_{d3} + k_{d5})$ are included in Table 3 and this choice affects the best-fit values of k_{b1} , k_{b2} , and k_{b3} as well as the best-fit values for k_{a1} , $(k_{a2} + k_{a4}K_L/K_{p1})$, $(k_{a3} + k_{a5}K_L/K_{p2})$, and k_{a6} determined from fitting the pH dependence of P1, Section 4.10.

Table 3 is divided into two sections. The first nine parameters in the table can be uniquely determined by fitting the spectroscopic, equilibrium, and kinetic data for imidazole binding to FixLH. The last eight parameters, beginning with $(k_{d3} + k_{d5})$, cannot be uniquely determined. We define these as contingent parameters, with their values dependent upon the choice made for $(k_{d3} + k_{d5})$. Although Table 3 does not provide a unique set of values for all parameters, it provides a self-consistent set that helps in understanding the mechanism of imidazole binding to FixLH.

With the values of pK_{p1}^* , pK_{p2}^* , k_{o1} , k_{o2} , and k_{o3} known from fitting P1/P3 and fixing the value of $k_d = (k_{d3} + k_{d5})$ at twice its minimum value, fitting P2 to Eq. (15) reduces to a problem of finding three adjustable parameters, k_{b1} , k_{b2} , and k_{b3} . Best-fit values for k_{b1} , k_{b2} , and k_{b3} are collected in Table 3 for the imidazole complexes of BjFixLH, SmFixLH, and SmFixLH(Y197F). For the BjFixLH imidazole encounter complex, k_b varies between 300 and $3000 s^{-1}$ depending upon the pH, Table 3. For the SmFixLH imidazole encounter complex, the maximum value of k_b varies between 70 and $23,000 s^{-1}$ and for the SmFixLH(Y197F) imidazole encounter complex, k_b varies between 74 and $2800 s^{-1}$. Plots of the pH dependence of k_b , calculated from Eq. (12), are shown in Figs. S18–S20. The effect of changing the value of $k_d = (k_{d3} + k_{d5})$ on the pH dependence of k_b is explored in the Supplementary Data.

4.10. pH dependence of the apparent association rate constant, P1

P1 is the only kinetic parameter that depends upon the association rate constant, k_a . In the encounter complex mechanism, $P1 = k_a k_o / (k_b + k_o)$ and value of k_a , as well as its pH dependence depends upon

the values of $P1$, k_o and k_b . Since $k_o = P1/P3$, the value of k_a can be found from the experimental values of $P1$, $P3$, and the calculated values of k_b , to Eq. (16).

$$k_a = P1 + P3 \cdot k_b \quad (16)$$

The value of k_b is not unique but depends upon the choice of value used for the dissociation rate constant, $k_d = k_{d3} + k_{d5}$. As a consequence, the calculated value of k_a will also depend upon the choice for k_d . A self-consistent, although not unique, set of parameters to explain the pH dependence of k_a is obtained by fitting the calculated values of k_a to Eq. (11). The best-fit values for k_{a1} , $(k_{a2} + k_{a4}K_L/K_{p1})$, $(k_{a3} + k_{a5}K_L/K_{p2})$, and k_{a6} for the *BjFixLH*, *SmFixLH* and *SmFixLH(Y197F)* imidazole reactions are collected in Table 3. Plots of the logarithm of k_a versus pH for the three FixLHs are shown in Figs. S21–S23.

As seen in Table 3, the dominant term in fitting the pH dependence of k_a is the $(k_{a3} + k_{a5}K_L/K_{p2})$, with values on the order of 10^7 to $10^8 \text{ M}^{-1} \text{ s}^{-1}$ for all three proteins. The effect of varying the value of k_d above its estimated minimum value on the pH dependence of k_b and subsequently, its effect in calculating k_a is explored in the Section 4.10 of the Supplementary Data. It is shown in the Supplementary Data that the $(k_{a3} + k_{a5}K_L/K_{p2})$ term is not very sensitive to the value of k_d . For the *BjFixLH* imidazole reaction, the $(k_{a3} + k_{a5}K_L/K_{p2})$ term decreases by less than a factor of 2 as the value of k_d increases from its minimum value to ten times its minimum value. This analysis supports the conclusion that formation of the FixLH imidazole encounter complex is very fast, approaching the rates of a diffusion-controlled reaction.

4.11. Comparison of cyanide binding to FixLH with other heme proteins

Cyanide binding to heme proteins has been extensively studied and Table S18 collects representative data from all major classes of heme proteins near pH 7. Observed association rate constants vary by more than 9 orders of magnitude, from $2.3 \times 10^{-3} \text{ M}^{-1} \text{ s}^{-1}$ to $2.5 \times 10^6 \text{ M}^{-1} \text{ s}^{-1}$ and observed dissociation rate constants vary by about 7 orders of magnitude, from $1.4 \times 10^{-6} \text{ s}^{-1}$ to 22 s^{-1} . The K_D values vary from $0.26 \mu\text{M}$ to 58 mM , over 5 orders of magnitude. Within this wide spectrum of values, the cyanide binding properties of the FixL heme domains are not unusual. The two FixL heme domains under study are among those proteins with intermediate affinities for cyanide at pH 7, with K_D values of 5.2 and $10.4 \mu\text{M}$ for *BjFixLH* and *SmFixLH*, respectively. The values of k_a are toward the slow end of those listed in Table S18. The k_a values are 18 and $14 \text{ M}^{-1} \text{ s}^{-1}$ for formation of the *BjFixLH* and *SmFixLH* cyanide complexes, respectively, at pH 7, some 5 orders of magnitude slower than the fastest cyanide binders in Table S18.

A major reason for the slow cyanide binding rate to FixLH is that the heme pocket is apolar. The pH studies show that the cyanide anion, rather than HCN, is preferentially bound by the heme domain of FixL (this work), as well as by most cytochromes, by EcDOSH, and by several hemoglobins that lack the distal histidine, Table S18. Looking at the data in Table S18, one is struck by the observation that the heme proteins with the smallest k_a values preferentially bind the anion while those with the largest k_a values preferentially bind HCN. Discrimination between the binding of HCN and CN^- is determined by the ability of HCN to ionize within the heme binding pocket [33,34]. For heme proteins with apolar heme pockets, it is faster for CN^- to diffuse into the heme pocket and bind to the iron than for HCN to diffuse into the pocket and undergo ionization prior to binding to the heme iron. Brancaccio et al. [33] have investigated the structural factors governing azide and cyanide binding to metMb and found that deprotonation of HCN was the major kinetic barrier to cyanide binding. The very rapid binding of HCN to yeast CcP, and the other peroxidases, is due to base catalysis of HCN ionization by a histidine residue in the distal heme pocket. The distal histidine in CcP is a critical residue in the catalytic mechanism, essential for activation of H_2O_2 . The distal histidine facilitates binding of the

peroxide anion to the heme iron through base catalysis. Mutagenesis studies show that there is a strong correlation between the rate of H_2O_2 activation and HCN binding and that these rates can be decreased by up to six orders of magnitude depending upon amino acid residues forming the heme pocket [35,36].

4.12. Comparison of imidazole binding to FixLH with other heme proteins

In general, imidazole binding to the heme proteins is more complex than that of cyanide, with conformational equilibria often involved in the binding as observed in FixLH. Table S19 presents an extensive compilation of K_D values for the imidazole complexes of heme proteins near pH 7. The K_D values range from $1.8 \mu\text{M}$ for a M96N mutant of *Rhodobacter capsulatus* cytochrome c_2 to no detectable binding for catalase and CooA, a range of at least 6 orders of magnitude. The apparent k_a range over five orders of magnitude, from $1.0 \times 10^6 \text{ M}^{-1} \text{ s}^{-1}$ for the H64A mutant of sperm whale metMb to $\sim 15 \text{ M}^{-1} \text{ s}^{-1}$ for horse cytochrome c . The apparent k_d values range over four orders of magnitude, from $1.2 \times 10^2 \text{ s}^{-1}$ for *Rhodobacter sphaeroides* cytochrome c_1 to $1.2 \times 10^{-2} \text{ s}^{-1}$ for sperm whale metMb(H64V). In many instances, the values of K_D do not equal k_d/k_a due to conformational equilibria, which are coupled to ligand binding.

The most extensive studies of imidazole binding have been to the globins and the c -type cytochromes. Mansy et al. [23] investigated the effects of mutating His-64, the distal histidine, and Leu-29 in sperm whale metMb on the binding of imidazole. They looked at 10 metMb mutants, four of which are included in Table S19, and found that they could alter the binding affinity by over 4 orders of magnitude, with K_D values ranging from $17 \mu\text{M}$ for the H64A mutant to 0.37 M for the L29F mutant at pH 7. The apparent k_a values also ranged over four orders of magnitude, from $1.0 \times 10^6 \text{ M}^{-1} \text{ s}^{-1}$ for the H64A mutant to $1.2 \times 10^2 \text{ M}^{-1} \text{ s}^{-1}$ for the L29F mutant. The apparent k_d values varied over 2 orders of magnitude, from 120 s^{-1} for H64V to 0.9 s^{-1} for H64Q. Mansy and colleagues concluded that the association rate constant was largely controlled by steric hindrance in the distal heme pocket while the dissociation rate constant was decreased significantly by distal site residues that could stabilize the heme-bound imidazole through hydrogen bonding.

The peroxidases, as a class, have very low affinity for imidazole [37]. Binding of imidazole to the heme in CcP is limited by conformational gating, precluding determination of the k_a and k_d for the imidazole complex [37]. The heme sensors, EcDOSH and CooA, also have very low affinity for imidazole. A lower limit of 1 M has been established for K_D of the EcDOSH-imidazole complex [38,39].

Compared to EcDOSH (an oxygen sensor) and CooA (a CO sensor), the binding of imidazole by FixLH is unusually strong with K_D values of $\sim 4 \text{ mM}$. This most likely reflects the fact that EcDOSH and CooA have hexa-coordinate hemes in their met forms and imidazole binding must displace the intrinsic heme ligand upon binding. In the context of all heme proteins, the imidazole affinity of FixLH is intermediate, some 3 orders of magnitude weaker than the strongest imidazole binders and some 3 orders of magnitude stronger than the weakest imidazole binders, Table S19. The intermediate imidazole affinity of FixLH is due to the large rate of binding, since the dissociation rates for the imidazole-FixLH complexes are among the fastest observed, with apparent rates of 51 and 91 s^{-1} for the *BjFixLH* and *SmFixLH*, respectively. The only complex listed in Table S19 with a faster dissociation rate is that of the H64V mutant of sperm whale metMb, which has a k_d of 120 s^{-1} .

The pH dependence of imidazole binding to FixLH is similar to that of metMb, with two ionizable groups in the protein affecting imidazole binding in both cases. In horse metMb, the group with lower $\text{p}K_a$ is identified as His-97 while in FixLH we have assigned this group to HP6. Both metMb and FixLH form hydroxy-ligated hemes at high pH and these alkaline forms react very slowly, if at all, with imidazole. Protonation of imidazole has a relatively small effect on the rate of imidazole binding to metMb [40,41] and a somewhat larger effect in FixLH (this work).

4.13. Ligand binding to FixLH and signal transduction

The primary function of the heme domain is to sense the presence of O₂ and transmit this information to the kinase domain, which ultimately leads to inhibition of transcription of the nitrogen-fixing genes, *nifA* and *fixK* [5]. The mechanism of signal transduction in the heme sensor proteins has been the subject of intense investigation over the last two decades. X-ray structures of ligand-free and ligated FixLH have provided structures of the initial and final states in the signal transduction process [10–18], while kinetic studies have provided information about the dynamics of conversion between the two states. Due to the photo-lability of the ferrous O₂, CO, and NO complexes, flash photolysis studies have provided a wealth of information on the early stages of ligand dissociation and rebinding. These results have recently been reviewed [42].

The major structural differences between deoxy-*Bj*FixLH and oxy-*Bj*FixLH [13] include movement of the heme iron into the plane of the porphyrin ring upon O₂ binding resulting in flattening of the heme, and movement of HP6 and HP7 relative to the heme plane. The latter movement changes the interaction between the heme propionates and residues in the F_α helix, the G_β strand, and the FG loop (residues 211 to 216). In the deoxy structure, HP6 is hydrogen bonded to the amide nitrogens of His-214 and Ile-215 (FG loop), while in the oxy structure HP6 interacts with His-214 (FG loop) and Arg-206 (F_α helix). HP7 hydrogens bonds to both His-214 and Arg-220 (G_β strand) in deoxy-FixLH, while in the oxy structure, HP7 only interacts with His-214. The changes in interaction of the heme propionates are associated with a large scale movement of the FG loop away from the heme in oxy-FixLH. In the distal heme pocket, Leu-236 and Ile-238 shift to accommodate the bound oxygen, and Arg-220, upon losing its interaction with HP7, rotates into the heme pocket and hydrogen bonds with the bound O₂. Binding of CO and NO cause significantly smaller structural changes [11,13,15] and also lower levels of inhibition of the catalytic activity of the kinase domain [42].

The proposed mechanism for signal transduction involving movement of the FG loop away from the heme involves changes in the interactions of both HP6 and HP7. The current study on the pH dependence of ligand binding to FixLH is consistent with the idea that changes in the protonation state of HP6 affects the rate and stability of both cyanide and imidazole binding to FixLH. In addition, deprotonation of HP6 increases the rate of heme pocket opening, allowing faster access to bulky ligands such as imidazole. The faster rate of heme pocket opening on going from low pH to neutral pH is consistent with weakening of the hydrogen bonding interactions between HP6 and the main chain amides of His-214 and Ile-215.

Time-resolved crystallographic studies of FixLH following CO photolysis of heme-bound CO showed that only two conformational states of the protein existed over the time frame of 1 μs to 10 ms, the ligand-bound state and the fully relaxed ligand-free state [17]. Upon photo-dissociation of bound CO, the protein structure went from the ligand-bound conformation to the fully relaxed ligand-free conformation within 1 μs. A 1.4 ms transient was also detected in this study, a transient due to CO rebinding and return to the ligand-bound protein conformation [17]. The structural differences between CO-bound and deoxy-*Bj*FixLH are much smaller than those between oxy- and deoxy-*Bj*FixLH and are concentrated in two regions of the protein [15]. The most prominent differences are associated with the movement of the Leu-236 side chain from its position directly over the heme iron in the deoxy state to accommodate bound CO. This results in an ~0.25 Å shift of the main chain atoms of Leu-236, also shifting the main chain atoms of Phe-252 and Val-253 to which Leu-236 hydrogen bonds. There are also small changes in the FG loop between Ile-215 and Gly-217. The backbone atoms of Ile-215 move about 0.3 Å relative to the deoxy structure and a hydrogen bond appears to be formed between HP6 and the backbone amide of Ile-216. There are no changes in the region of HP7 and Arg-220 indicating that the salt bridge between Arg-220 and HP7 remains intact in CO-FixLH.

Limited structural information is available from time resolved UV resonance Raman (UVRR) spectroscopy following photolysis of CO and O₂ [43]. Intensity changes in a band at 345 cm⁻¹ attributed to formation of the salt bridge between HP7 and Arg-214 in *Sm*FixL (Arg-220 in *Bj*FixLH) decayed with time constants of 0.3 μs and 1 μs in FixLH and full length FixL, respectively. A second band at 380 cm⁻¹, involving heme propionate methylene deformation and whose intensity is sensitive to surrounding residues, decayed with time constants of about 1 μs and 3 μs in the heme domain and full length FixL, respectively. This step was attributed to changes in the interaction between HP6 and the FG loop residues, Ile-209 and Ile-210 (Ile-215 and Ile-216 in *Bj*FixLH) and movement of Ile-209 into the space vacated by the departing O₂. If these interpretations of the intensity changes are correct, the UVRR data suggest that movement of the FG loop and residues in the distal pocket occur on the μs time scale following dissociation of the ligand. In the photo-dissociation studies, transients in the ms time frame were also observed and attributed to ligand rebinding. In a more recent study [44], a Raman band attributed to Tyr-201 in *Sm*FixL (Tyr-207 in *Bj*FixLH) increased in amplitude with a time constant of 0.1 μs following O₂ photolysis and was associated with changes in the F_α helix prior to movement of the FG loop.

The flash photolysis studies show that the conformational changes in FixLH can occur in less than 1 μs following CO and O₂ dissociation and that in the forward direction, conformational changes occur simultaneously with ligand binding, i.e., there is no conformational impediment to CO or O₂ binding under the typical experimental conditions.

Binding of both cyanide and imidazole convert FixL from the catalytically-active five-coordinate, high-spin met conformation to the inactive ligand-bound, six-coordinate, low-spin conformation [9–11, 13,42]. Although the structures of the cyanide and imidazole complexes are not identical [13], they both share in the movement of FG loop away from the heme. The only potential barrier to cyanide binding to the heme iron would be the movement of the three hydrophobic residues in the distal heme pocket, primarily Ile-238, away from the heme iron. The time-resolved x-ray and UVRR studies show that this type of movement can occur in less than 1 μs, over two orders of magnitude faster than the fastest rate of cyanide binding we observed in this study, Figs. S7 and S8. As a consequence of the very fast conformational changes, the binding of cyanide appears as a simple monophasic ligand binding reaction.

Imidazole binding is much more interesting due to saturation of the observed rate constant at high imidazole concentrations, Fig. S10. The limiting rate is almost certainly due to the movement of amino acid residues blocking access to the heme iron. In both the conformational gating and encounter complex mechanisms, Section 4.6, the limiting rate constant is defined as k_o , the rate of heme pocket opening. At neutral pH, this rate is 460 s⁻¹ for *Bj*FixLH and 1270 s⁻¹ for *Sm*FixLH, characteristic times of 2.2 ms and 0.79 ms, respectively. Rates in the ms region have been observed in the flash photolysis studies of CO- and O₂-ligated FixLH and these have been attributed to ligand rebinding [17,43].

The major barrier to binding imidazole to the heme iron is the location of Ile-215, Leu-236, and Ile-238 in the distal heme pocket. The side chain of Ile-238 appears to rotate out of the way of the imidazole and there is a 2.2 Å displacement of Ile-215 out of the heme pocket. The carbonyl of Ile-215 hydrogen bonds to a water molecule, which in turn hydrogen bonds to the imidazole ring. In addition, the salt bridge between Arg-220 and HP7 in the metFixLH structure is disrupted. The Arg-220 side chain does not hydrogen bond to the bound ligand in the imidazole complex but rotates to the surface of the molecule extending into solution. The orientation of the main chain atoms in the FG loop of the imidazole-*Bj*FixLH complex is similar to the orientation of the FG loops in oxy- and cyanomet-*Bj*FixLH. Since the largest differences between the imidazole complex and the oxy- and cyanomet-FixLH complexes are in the Ile-215 and Arg-220 side chain positions, a reasonable hypothesis is that the rate limiting step in imidazole binding is associated with movement of these two residues.

For binding of small diatomic molecules such as O₂, CO, and CN[−], the conformational changes in the protein occur simultaneously with ligand binding indicating that the protein dynamics are sufficiently fast to accommodate the ligand. In the case of bulky ligands such as imidazole, the protein conformation must change before the ligand can bind and these conformational changes can become rate limiting. Finally, it should be noted that the rate of any protein conformation change associated with ligand binding need not occur on the same time scale as the rate of protein relaxation following ligand dissociation.

5. Conclusions

5.1. Cyanide binding to FixLH

The apolar heme pocket of FixLH discriminates between HCN and CN[−], with the binding of CN[−] more than three orders of magnitude faster than that of HCN. Two ionizable groups in FixLH influence binding of CN[−]. The more acidic group has been identified as HP6, which is hydrogen-bonded to the amide nitrogens of both His-214 and Ile-215, and coupled to the conformational shift in the FG loop. The pK_a of HP6 is 7.6 in ligand-free FixLH and ionization of HP6 reduces the rate of cyanide binding two-fold due to electrostatic repulsion between the negatively-charged carboxylate and the cyanide anion. The second ionization is due to the formation of hydroxy-FixLH with a pK_a near 9.6 in both *BjFixLH* and *SmFixLH*. Hydroxy-FixLH is at least 30-fold less reactive toward CN[−] than FixLH. The maximum observed values for the association rate constant are (443 ± 8) M^{−1} s^{−1} for *BjFixLH* and (252 ± 61) M^{−1} s^{−1} for *SmFixLH*, both at pH 9.5, occurring approximately midway between the pK_{as} for ionization of HCN and formation of hydroxy-FixLH. Binding of cyanide is so slow that conformational dynamics do not limit the rate of cyanide binding.

There is only one reactive form of cyano-FixLH between pH 5 and 11 and the rate of cyanide dissociation from the complex is independent of pH, with observed dissociation rate constants of (1.2 ± 0.3) × 10^{−4} s^{−1} and (1.7 ± 0.3) × 10^{−4} s^{−1} for the *BjFixLH* and *SmFixLH* complexes, respectively. The dissociation rate constant increases below pH 5 due to the protonation of HP6. The pK_a of HP6 is less than 5 in the cyano complex.

Experimental values of K_D were determined at integral pH values. The strongest binding occurred at pH 9, with K_D values of 0.15 ± 0.09 μM and 0.50 ± 0.20 μM for the cyano complexes of *BjFixLH* and *SmFixLH*, respectively.

5.2. Imidazole binding to FixLH

The picture that emerges from this study of imidazole binding to FixLH is that imidazole binds rapidly to form an encounter complex, with imidazole associated with the protein but not bound to the heme. Conformational changes within the encounter complex open the distal heme pocket with rates of 460 s^{−1} for the *BjFixLH* complex and 1270 s^{−1} for the *SmFixLH* complex at pH 7 allowing imidazole to bind to the heme iron. We attribute the rates of heme pocket opening with the movements of the side-chains of Ile-215 (FG loop) and Arg-220 (G_β strand) away from the heme, converting FixLH from its catalytically active conformation [10] to an inactive conformation [11]. In the imidazole complex, the conformational changes associated with imidazole binding are considerably slower than the rates of FG loop movement during the photolysis of O₂ [43]. However, the movement of the Ile-215 and Arg-220 side-chains is much larger between met-FixLH and the imidazole complex than between deoxy- and oxy-FixLH [13] and could result in a slower rate of reorientation.

Due to the coupling of the conformational changes with imidazole binding, only apparent association and dissociation rate constants for the imidazole-FixLH complex can be determined, which in both cases are minimum values. The apparent association rate constant for imidazole binding to *BjFixLH* varies from (2.0 ± 0.9) × 10³ M^{−1} s^{−1} at pH 5 to

(5.0 ± 0.3) × 10⁴ M^{−1} s^{−1} at pH 8.5, decreasing to (7.4 ± 2.7) × 10³ M^{−1} s^{−1} at pH 11. The pH dependence indicates that FixLH discriminates between the protonated and unprotonated forms of imidazole, binding neutral imidazole some 25 times faster than the imidazolium cation to *BjFixLH* and 4 times faster to *SmFixLH*. Hydroxylation of FixLH does not have as large an impact on the binding of imidazole as it does on the binding of cyanide. The binding of imidazole to hydroxy-FixLH is only 2-times slower than binding to the penta-coordinate met form of *SmFixLH* and 7-times slower than to met-*BjFixLH*.

The apparent dissociation rate constant for the imidazole-FixLH complex is essentially independent of pH just as for the cyanide complex, with an average value of 73 ± 19 s^{−1} between pH 5 and 11 for the *BjFixLH* complex and 77 ± 14 s^{−1} for the *SmFixLH* complex. The very small pH dependence seen for *BjFixLH* imidazole complex can be accounted for based on the coupling of the conformational changes with imidazole dissociation.

The rate of heme pocket opening is pH dependent and appears to be affected by both the ionization of HP6 and formation of hydroxy-FixLH. The maximum rate of heme pocket opening for *BjFixLH* is 680 s^{−1} at pH 9, decreasing to 270 s^{−1} at pH 5 and 170 s^{−1} at pH 11. For *SmFixLH*, the maximum rate of heme pocket opening is 1270 s^{−1} at pH 7, decreasing to 290 s^{−1} at pH 5 and 100 s^{−1} at pH 11.

5.3. Effect of the Y197F mutation on imidazole binding to *SmFixLH*

The Y197F mutation of *SmFixLH* affects the kinetic parameters for imidazole binding to some extent although the changes are not large. The apparent association rate constant for imidazole binding to *SmFixLH*(Y197F) varies from (3.4 ± 2.1) × 10³ M^{−1} s^{−1} at pH 5 to (1.8 ± 0.5) × 10⁵ M^{−1} s^{−1} at pH 9.0, decreasing to (2.5 ± 2.2) × 10³ M^{−1} s^{−1} at pH 11. Between pH 6 and 10, the apparent imidazole association rate constant (P1) for the Y197F mutant averages about 50% faster than that of *SmFixLH*. The apparent dissociation rate constant for the Y197F mutant is 95 ± 24 s^{−1} over the pH range 5 to 11 compared to 77 ± 14 s^{−1} for *SmFixLH*.

The biggest effect of the Y197F mutation is on the rate of heme pocket opening, providing support for the idea of protein destabilization in the Y197F mutant. The rate of heme pocket opening is faster for the Y197F mutant than for *SmFixLH* over the entire pH range with the largest differences at low pH rather than at alkaline pH. Tyr-197 is located in the F_α helix, three residues from the proximal heme ligand His-194. The phenolic group of Tyr-197 is hydrogen bonded to the carboxylate group of Asp-190, also located in the F_α helix. Disruption of this hydrogen bond could destabilized the F_α helix to some extent and allow the side chains of both Phe-197 and Asp-190 to adopt alternative orientations, perhaps destabilizing the FG loop.

5.4. Binding of 4-nitroimidazole to *SmFixLH*

Adding the electron-withdrawing nitro group to imidazole substantially increases the acidity of both nitrogens in the ring. The apparent pK_{as} for the imidazolium/imidazole and the imidazole/imidazolate ionizations are −0.05 and 8.96, respectively [32]. This means that the ligand will be predominantly neutral between pH 5 and 8.96 and predominantly negatively charged between pH 8.96 and 11 in contrast with imidazole, which is positively charged below pH 7 and neutral above pH 7. Unfortunately, the limited solubility of 4-nitroimidazole did not allow studies at high enough concentration to observe saturation of the binding rate. We were only able to obtain values for the apparent association and dissociation rate constants. Both apparent rate constants average about 40-fold smaller for 4-nitroimidazole binding to *SmFixLH* than for imidazole binding. Interestingly, at pH 9, the apparent equilibrium dissociation constants for imidazole and 4-nitroimidazole complexes are essentially the same, 0.26 mM and 0.23 mM, respectively.

Acknowledgments

Professor James Satterlee (deceased), Washington State University, performed the MALDI-TOF mass spectroscopic analysis of purified *BjFixLH* and *SmFixLH*. This work was supported in part by the National Institutes of Health through grant R15 GM59740.

Appendix A. Supplementary data

Supplementary data to this article can be found online at <http://dx.doi.org/10.1016/j.jinorgbio.2015.10.003>.

References

- [1] E. Antonini, M. Brunori, Hemoglobin and Myoglobin in Their Reactions with Ligands, North-Holland, Amsterdam, 1971.
- [2] K.R. Rodgers, Heme-based sensors in biological systems, *Curr. Opin. Chem. Biol.* 3 (1999) 158–167.
- [3] C.W. Ronson, B.T. Nixon, F.M. Ausubel, Conserved domains in bacterial regulatory proteins that respond to environmental stimuli, *Cell* 49 (1987) 579–581.
- [4] M. David, M.-L. Daveran, J. Batut, A.A. Dedieu, O. Domergue, J. Ghai, C. Hertig, P. Boistard, D. Kahn, Cascade regulation of *nif* gene expression in *Rhizobium meliloti*, *Cell* 54 (1988) 671–683.
- [5] E.K. Monson, M. Weinstein, G.S. Ditta, D.R. Helsinki, The FixL protein of *Rhizobium meliloti* can be separated into a heme-binding oxygen-sensing domain and a functional C-terminal kinase domain, *Proc. Natl. Acad. Sci. U. S. A.* 89 (1992) 4280–4284.
- [6] A.F. Lois, G.S. Ditta, D.R. Helsinki, The oxygen sensor protein FixL of *Rhizobium meliloti* is a membrane protein containing four possible transmembrane segments, *J. Bacteriol.* 175 (1993) 1103–1109.
- [7] M.A. Gilles-Gonzalez, G. Gonzalez, Regulation of the kinase activity of heme protein FixL from the two-component system FixL/FixJ of *Rhizobium meliloti*, *J. Biol. Chem.* 268 (1993) 16293–16297.
- [8] D. Anthamatten, H. Hennecke, The regulatory status of the *fixL*- and *fixJ*-like genes in *Bradyrhizobium japonicum* may be different from that in *Rhizobium meliloti*, *Mol. Gen. Genet.* 225 (1991) 38–48.
- [9] M.A. Gilles-Gonzalez, G. Gonzalez, M.F. Perutz, Kinase activity of oxygen sensor FixL depends on the spin state of its heme iron, *Biochemistry* 34 (1995) 232–236.
- [10] W. Gong, B. Hao, S.S. Mansy, G. Gonzalez, M.A. Gilles-Gonzalez, M.K. Chan, Structure of a biological oxygen sensor: a new mechanism for heme-driven signal transduction, *Proc. Natl. Acad. Sci. U. S. A.* 95 (1998) 15177–15182.
- [11] W. Gong, B. Hao, M.K. Chan, New mechanistic insights from structural studies of the oxygen-sensing domain of *Bradyrhizobium japonicum* FixL, *Biochemistry* 39 (2000) 3955–3962.
- [12] H. Miyatake, M. Mukai, S. Park, S. Adachi, K. Tamura, H. Nakamura, K. Nakamura, T. Tsuchiya, T. Iizuka, Y. Shiro, Sensory mechanism of oxygen sensor FixL from *Rhizobium meliloti*: crystallographic, mutagenesis and resonance Raman spectroscopic studies, *J. Mol. Biol.* 301 (2000) 415–431.
- [13] B. Hao, C. Isaza, J. Arndt, M. Soltis, M.K. Chan, Structure-based mechanism of O₂ sensing and ligand discrimination by the FixL heme domain of *Bradyrhizobium japonicum*, *Biochemistry* 41 (2002) 12952–12958.
- [14] C.M. Dunham, E.M. Dioum, J.R. Tuckerman, G. Gonzalez, W.G. Scott, M.A. Gilles-Gonzalez, A distal arginine in oxygen-sensing heme-PAS domains is essential to ligand binding, signal transduction, and structure, *Biochemistry* 42 (2003) 7701–7708.
- [15] J. Key, K. Moffat, Crystal structures of deoxy and CO-bound *bjFixLH* reveal details of ligand recognition and signaling, *Biochemistry* 44 (2005) 4627–4635.
- [16] M.A. Gilles-Gonzalez, A.I. Caceres, E.H.S. Sousa, D.R. Tomchick, C.A. Brautigam, C. Gonzalez, M. Machius, A proximal arginine R206 participates in switching of the *Bradyrhizobium japonicum* FixL oxygen sensor, *J. Mol. Biol.* 360 (2006) 80–89.
- [17] J. Key, V. Šrajer, R. Pahl, K. Moffat, Time-resolved crystallographic studies of the heme domain of the oxygen sensor FixL: structural dynamics of ligand rebinding and their relation to signal transduction, *Biochemistry* 46 (2007) 4706–4715.
- [18] R.A. Ayers, K. Moffat, Changes in quaternary structure in the signaling mechanisms of pas domains, *Biochemistry* 47 (2008) 12078–12086.
- [19] M.A. Gilles-Gonzalez, G. Gonzalez, M.F. Perutz, L. Kiger, M.C. Marden, C. Poyart, Heme-based sensors, exemplified by the kinase FixL, are a new class of heme protein with distinctive ligand binding and autoxidation, *Biochemistry* 33 (1994) 8067–8073.
- [20] L. Kiger, F. Stetzkowski-Marden, C. Poyart, M.C. Marden, Correlation of carbon monoxide association rates and the position of absorption band III in hemoproteins, *Eur. J. Biochem.* 228 (1995) 665–668.
- [21] W.C. Winkler, G. Gonzalez, J.B. Wittenberg, R. Hille, N. Dakappagari, A. Jacob, L.A. Gonzalez, M.A. Gilles-Gonzalez, Nonsteric factors dominate binding of nitric oxide, azide, imidazole, cyanide and fluoride to the rhizobial heme-based oxygen sensor FixL, *Chem. Biol.* 3 (1996) 841–850.
- [22] K.R. Rodgers, G.S. Lukat-Rodgers, J.A. Barron, Structural basis for ligand discrimination and response initiation in the heme-based oxygen sensor FixL, *Biochemistry* 35 (1996) 9539–9548.
- [23] S.S. Mansy, J.S. Olson, G. Gonzalo, M.A. Gilles-Gonzalez, Imidazole is a sensitive probe of steric hindrance in the distal pocket of oxygen-binding heme proteins, *Biochemistry* 37 (1998) 12452–12457.
- [24] K.R. Rodgers, L. Tang, G.S. Lukat-Rodgers, N.L. Wengenack, Insights into the signal transduction mechanism of *RmFixL* provided by carbon monoxide recombination kinetics, *Biochemistry* 40 (2001) 12932–12942.
- [25] U. Liebl, L. Bouzahir-Sima, M. Négrerie, J.-L. Martin, M.H. Vos, Ultrafast ligand rebinding in the heme domain of the oxygen sensors FixL and Dos: general regulatory implications for heme-based sensors, *Proc. Natl. Acad. Sci. U. S. A.* 99 (2002) 12771–12776.
- [26] J. Mikšová, C. Suquet, J.D. Satterlee, R.W. Larsen, Characterization of conformational changes coupled to ligand photodissociation from the heme binding domain of FixL, *Biochemistry* 44 (2005) 10028–10036.
- [27] A. Jasaitis, K. Hola, L. Bouzahir-Sima, J.-C. Lambry, V. Bolland, M.H. Vos, U. Liebl, Role of distal arginine in early sensing intermediates in the heme domain of the oxygen sensor FixL, *Biochemistry* 45 (2006) 6018–6026.
- [28] E.A. Berry, B.L. Trumpower, Simultaneous determination of hemes a, b, and c from pyridine hemeochrome spectra, *Anal. Biochem.* 161 (1987) 1–15.
- [29] W.J. Eilbeck, M.S. West, Thermochemical studies of vitamin B₁₂. Part II. Thermodynamic data for the interaction of imidazole and methylimidazoles with aquocobalamin (vitamin B₁₂), *J. Chem. Soc. Dalton Trans.* 274–278 (1976).
- [30] R.M. Izatt, J.J. Christensen, R.T. Pack, R. Bench, Thermodynamics of metal-cyanide coordination. I. pK, ΔH°, and ΔS° values as a function of temperature for hydrocyanic acid dissociation in aqueous solution, *Inorg. Chem.* 1 (1962) 828–831.
- [31] G.S. Lukat-Rodgers, J.L. Rexine, K.R. Rodgers, Heme speciation in alkaline ferric FixL and possible tyrosine involvement in the signal transduction pathway for regulation of nitrogen fixation, *Biochemistry* 37 (1998) 13543–13552.
- [32] K.C. Taylor, L.B. Vitello, J.E. Erman, 4-nitroimidazole binding to horse metmyoglobin: evidence for preferential anion binding, *Arch. Biochem. Biophys.* 382 (2000) 284–295.
- [33] A. Brancaccio, F. Cutruzzola, C.T. Allocatelli, M. Brunori, S.J. Smerdon, A.J. Wilkinson, Y. Dou, D. Keenan, M. Ikeda-Saito, R.E. Brantly Jr., J.S. Olson, Structural factors governing azide and cyanide binding to mammalian metmyoglobins, *J. Biol. Chem.* 269 (1994) 13843–13853.
- [34] Y. Dou, J.S. Olson, A.J. Wilkinson, M. Ikeda-Saito, Mechanism of hydrogen cyanide binding to myoglobin, *Biochemistry* 35 (1996) 7107–7113.
- [35] A. Bidwai, M. Witt, M. Foshay, L.B. Vitello, J.D. Satterlee, J.E. Erman, Cyanide binding to cytochrome c peroxidase (H52L), *Biochemistry* 42 (2003) 10764–10771.
- [36] A.K. Bidwai, C. Meyen, H. Kilheeny, D. Wroblewski, L.B. Vitello, J.E. Erman, Apolar distal pocket mutants of yeast cytochrome c peroxidase: hydrogen peroxide reactivity and cyanide binding of the triAla, triVal, and triLeu variants, *Biochim. Biophys. Acta* 1834 (2013) 137–148.
- [37] J.E. Erman, D. Chinchilla, J. Studer, L.B. Vitello, Binding of imidazole, 1-methylimidazole and 4-nitroimidazole to yeast cytochrome c peroxidase (CcP) and the distal histidine mutant, CcP(H52L), *Biochim. Biophys. Acta* 1854 (2015) 869–881.
- [38] M. Watanabe, T. Matsui, Y. Sasakura, I. Sagami, T. Shimizu, unusual cyanide binding to a heme-regulated phosphodiesterase from *Escherichia coli*: effect of met95 mutations, *Biochem. Biophys. Res. Commun.* 299 (2002) 169–172.
- [39] A.K. Bidwai, E.Y. Ok, J.E. Erman, pH dependence of cyanide binding to the ferric heme domain of the direct oxygen sensor from *Escherichia coli* and the effect of alkaline denaturation, *Biochemistry* 47 (2008) 10458–10470.
- [40] D.E. Goldsack, W.S. Eberlin, R.A. Alberty, Temperature jump studies of sperm whale metmyoglobin. III. Effect of heme-linked groups on ligand binding, *J. Biol. Chem.* 241 (1966) 2653–2660.
- [41] J. Lin, L.B. Vitello, J.E. Erman, Imidazole binding to horse myoglobin: dependence upon pH and ionic strength, *Arch. Biochem. Biophys.* 352 (1998) 214–228.
- [42] U. Liebl, J.-C. Lambry, M.H. Vos, Primary processes in heme-based sensor proteins, *Biochim. Biophys. Acta* 1834 (2013) 1684–1692.
- [43] Y. Hiruma, A. Kikuchi, A. Tanaka, Y. Shiro, Y. Mitzutani, Resonance Raman observation of the structural dynamics of FixL on signal transduction and ligand discrimination, *Biochemistry* 46 (2007) 6086–6096.
- [44] S. Yano, H. Ishikawa, M. Mizuno, H. Nakamura, Y. Shiro, Y. Mitzutani, Ultraviolet resonance Raman observations of the structural dynamics of *Rhizobial* oxygen sensor FixL on ligand recognition, *J. Phys. Chem. B* 117 (2013) 15786–15791.